

Accepted Manuscript

Plant-wide modelling of phosphorus transformations in wastewater treatment systems: Impacts of control and operational strategies

K. Solon, X. Flores-Alsina, C. Kazadi Mbamba, D. Ikumi, E.I.P. Volcke, C. Vaneekhaute, G. Ekama, P.A. Vanrolleghem, D.J. Batstone, K.V. Gernaey, U. Jeppsson

PII: S0043-1354(17)30082-9

DOI: [10.1016/j.watres.2017.02.007](https://doi.org/10.1016/j.watres.2017.02.007)

Reference: WR 12676

To appear in: *Water Research*

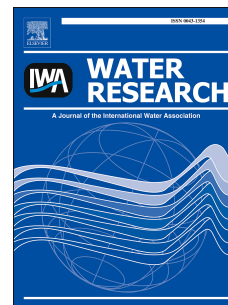
Received Date: 5 October 2016

Revised Date: 2 February 2017

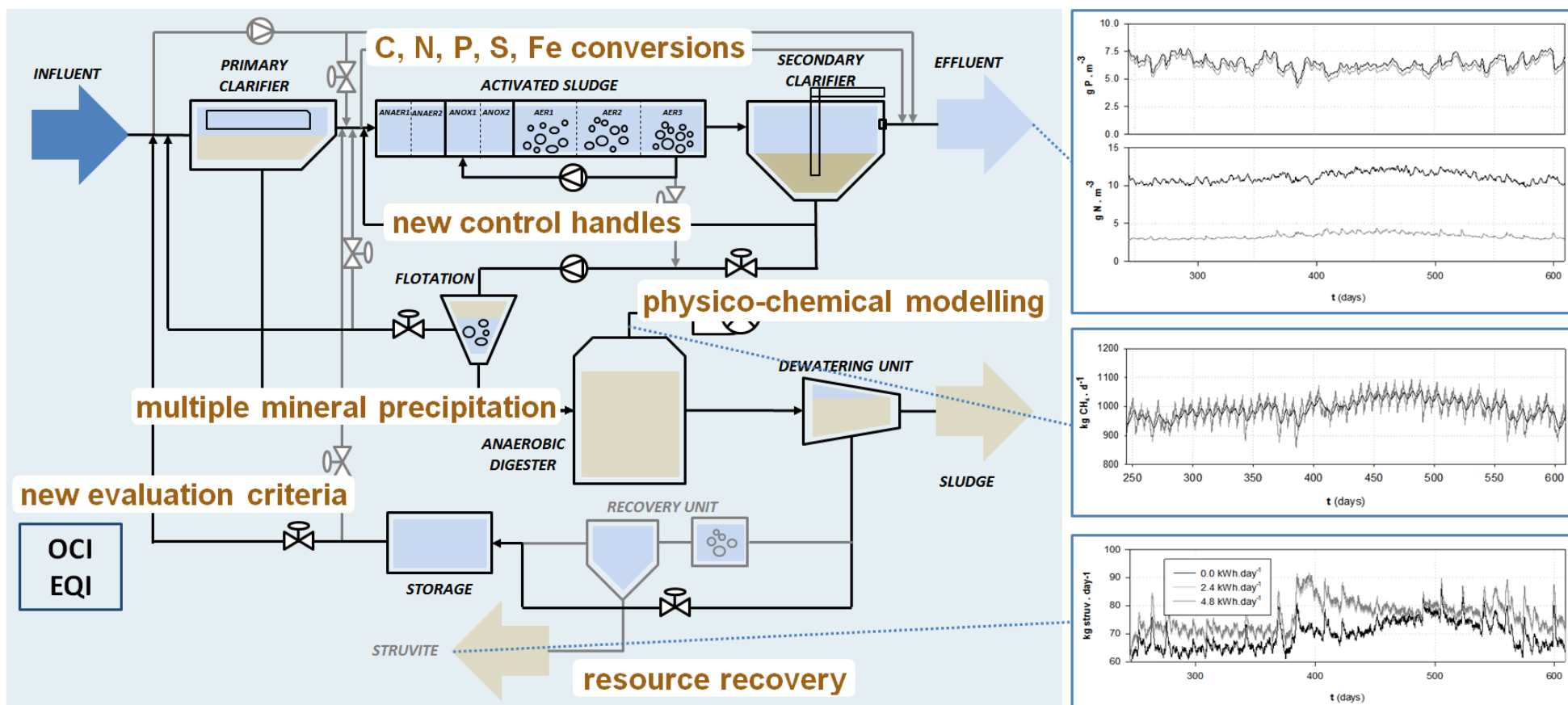
Accepted Date: 3 February 2017

Please cite this article as: Solon, K., Flores-Alsina, X., Kazadi Mbamba, C., Ikumi, D., Volcke, E.I.P., Vaneekhaute, C., Ekama, G., Vanrolleghem, P.A., Batstone, D.J., Gernaey, K.V., Jeppsson, U., Plant-wide modelling of phosphorus transformations in wastewater treatment systems: Impacts of control and operational strategies, *Water Research* (2017), doi: 10.1016/j.watres.2017.02.007.

This is a PDF file of an unedited manuscript that has been accepted for publication. As a service to our customers we are providing this early version of the manuscript. The manuscript will undergo copyediting, typesetting, and review of the resulting proof before it is published in its final form. Please note that during the production process errors may be discovered which could affect the content, and all legal disclaimers that apply to the journal pertain.



GRAPHICAL ABSTRACT



1 **Plant-wide modelling of phosphorus transformations in wastewater**
ACCEPTED MANUSCRIPT
2 **treatment systems: Impacts of control and operational strategies**

3
4 K. Solon¹, X. Flores-Alsina², C. Kazadi Mbamba³, D. Ikumi⁴, E.I.P. Volcke⁵, C. Vaneckhaute⁶, G. Ekama⁴,
5 P.A. Vanrolleghem⁷, D.J. Batstone³, K.V. Gernaey², U. Jeppsson^{1*}
6

1 ¹ Division of Industrial Electrical Engineering and Automation, Department of Biomedical Engineering,
Lund University, Box 118, SE-221 00 Lund, Sweden.

2 ² CAPEC-PROCESS Research Center, Department of Chemical and Biochemical Engineering, Technical
University of Denmark, Building 229, DK-2800 Kgs. Lyngby, Denmark.

3 ³ Advanced Water Management Centre, The University of Queensland, St Lucia, Brisbane, Queensland
4072, Australia.

4 ⁴ Water Research Group, Department of Civil Engineering, University of Cape Town, Rondebosch 7700,
South Africa.

5 ⁵ Department of Biosystems Engineering, Ghent University, Coupure links 653, B-9000 Gent, Belgium.

6 ⁶ BioEngine, Department of Chemical Engineering, Université Laval, Québec, QC, Canada, G1V 0A6.

7 ⁷ modelEAU, Département de Génie Civil et de Génie des Eaux, Université Laval, Québec, QC, Canada,
G1V 0A6.

8 **Corresponding author:*

9 Ulf Jeppsson

10 Division of Industrial Electrical Engineering and Automation (IEA)

11 Department of Biomedical Engineering

12 Lund University, Box 118, SE-221 00

13 Lund, Sweden

14 Phone: +46 46 222 92 87

15 Fax: +46 46 14 21 14

16 e-mail: ulf.jeppsson@iea.lth.se

A	Alternative
AD	Anaerobic digestion
ADM1	Anaerobic Digestion Model No. 1
AER	Aerobic section
ANAER	Anaerobic section
ANOX	Anoxic section
ASM	Activated Sludge Model
ASM2d	Activated Sludge Model No. 2d
BOD	Biological oxygen demand
BSM2	Benchmark Simulation Model No. 2
CBIM	Continuity-based interfacing method
COD	Chemical oxygen demand
CONV _{AD-AS}	Conversion ADM1 – ASM2d interface
CONV _{AS-AM}	Conversion ASM2d – ADM1 interface
DO	Dissolved oxygen
EQI	Effluent quality index
Fe	Iron
GAO	Glycogen accumulating organisms
G_{CH_4}	Methane production rate (gas) (ADM1) (kg.day ⁻¹)
G_{CO_2}	Carbon dioxide production rate (gas) (ADM1) (kg.day ⁻¹)
G_{H_2}	Hydrogen production rate (gas) (ADM1) (kg.day ⁻¹)
G_{H_2S}	Hydrogen sulfide production rate (gas) (ADM1) (kg.day ⁻¹)
MMP	Multiple mineral precipitation
OCI	Operational cost index
P	Phosphorus
PAO	Phosphorus accumulating organisms
PHA	Polyhydroxyalkanoates
PP	Polyphosphates
PRIM	Primary clarifier
PROCESS _{AD-AS}	Process ADM1– ASM2d interface
PROCESS _{AS-AD}	Process ASM2d – ADM1 interface
Q_{intr}	Internal recycle flow rate (between AER and ANOX) (m ³ .day ⁻¹)
S	Sulfur
SEC2	Secondary clarifier
SI	Saturation index
SRB	Sulfate-reducing bacteria
STRIP	Stripping unit
S_A	Acetate (ASM2d) (g COD.m ⁻³)
S_{aa}	Amino acids (ADM1) (kg COD.m ⁻³)

S_{ac}	Total acetic acid (ADM1) (kg COD.m ⁻³)
S_{an}	Anions (ADM1) (kmol.m ⁻³)
S_{bu}	Total butyric acid (ADM1) (kg COD.m ⁻³)
S_{Ca}	Calcium (ASM2d, ADM1) (g.m ⁻³) (kmol.m ⁻³)
S_{cat}	Soluble cations (ADM1) (kmol.m ⁻³)
S_{Cl}	Chloride (ASM2d, ADM1) (g.m ⁻³) (kmol.m ⁻³)
S_F	Fermentable substrate (ASM2d) (g COD.m ⁻³)
S_{fa}	Fatty acids (ADM1) (kg COD.m ⁻³)
$S_{Fe^{2+}}$	Iron (II) (ASM2d, ADM1) (g.m ⁻³) (kmol.m ⁻³)
$S_{Fe^{3+}}$	Iron (III) (ASM2d, ADM1) (g.m ⁻³) (kmol.m ⁻³)
S_{H_2}	Hydrogen (ADM1) (kg COD.m ⁻³)
S_{IC}	Inorganic carbon (ADM1) (kmol.m ⁻³)
S_{IN}	Inorganic nitrogen (ADM1) (kmol.m ⁻³)
S_{IP}	Inorganic phosphorus (ADM1) (kmol.m ⁻³)
S_{IS}	Inorganic total sulfides (ADM1) (kg COD.m ⁻³)
S_K	Potassium (ASM2d, ADM1) (g.m ⁻³) (kmol.m ⁻³)
S_{Mg}	Magnesium (ASM2d, ADM1) (g.m ⁻³) (kmol.m ⁻³)
S_{Na}	Sodium (ASM2d, ADM1) (g.m ⁻³) (kmol.m ⁻³)
S_{NH_x}	Ammonium plus ammonia nitrogen (ASM2d) (g.m ⁻³)
S_{NO_x}	Nitrate plus nitrite (ASM2d) (g.m ⁻³)
S_{pro}	Total propionic acid (ADM1) (kg COD.m ⁻³)
S_{PO_4}	Phosphate (ASM2d) (g.m ⁻³)
S_{su}	Sugars (ADM1) (kg COD.m ⁻³)
S_{S_0}	Elemental sulfur (ADM1) (kmol.m ⁻³)
S_{SO_4}	Sulfate (ASM2d, ADM1) (g.m ⁻³) (kmol.m ⁻³)
S_{va}	Total valeric acid (ADM1) (kg COD.m ⁻³)
THK/FLOT	Thickener/flotation
TIV	Time in violation
TKN	Total Kjeldahl nitrogen
TN	Total nitrogen
TP	Total phosphorus
TSS	Total suspended solids
VFA	Volatile fatty acids
WRRF	Water resource recovery facility
WWTP	Wastewater treatment plant
X_A	Autotrophic biomass (ASM2d) (g COD.m ⁻³)
X_{ac}	Acetate degraders (ADM1) (kg COD.m ⁻³)
X_{AlPO_4}	Aluminum phosphate (ASM2d, ADM1) (g.m ⁻³) (kmol.m ⁻³)
X_B	Total biomass (ADM1) (kg COD.m ⁻³)
X_c	Composite material (ADM1) (kg COD.m ⁻³)
X_{C4}	Butyrate and valerate degraders (ADM1) (kg COD.m ⁻³)

X_{CaCO_3}	Calcite (ASM2d, ADM1) (g.m^{-3}) (kmol.m^{-3})
$X_{\text{CaCO}_{3a}}$	Aragonite (ASM2d, ADM1) (g.m^{-3}) (kmol.m^{-3})
$X_{\text{Ca}_3(\text{PO}_4)_2}$	Amorphous calcium phosphate (ASM2d, ADM1) (g.m^{-3}) (kmol.m^{-3})
$X_{\text{Ca}_5(\text{PO}_4)_3(\text{OH})}$	Hydroxylapatite (ASM2d, ADM1) (g.m^{-3}) (kmol.m^{-3})
$X_{\text{Ca}_8\text{H}_2(\text{PO}_4)_6}$	Octacalcium phosphate (ASM2d, ADM1) (g.m^{-3}) (kmol.m^{-3})
X_{ch}	Carbohydrates (ADM1) (kg COD.m^{-3})
X_{FePO_4}	Iron (III) phosphate (ASM2d, ADM1) (g.m^{-3}) (kmol.m^{-3})
$X_{\text{Fe}_3(\text{PO}_4)_2}$	Iron (II) phosphate (ASM2d, ADM1) (mol.L^{-1}) (kmol.m^{-3})
X_{FeS}	Iron sulfide (ASM2d, ADM1) (mol.L^{-1}) (kmol.m^{-3})
X_{H}	Heterotrophic biomass (ASM2d) (g COD.m^{-3})
$X_{\text{HFO-H}}$	Hydrous ferric oxide with high number of active sites (ASM2d, ADM1) (g.m^{-3}) (kmol.m^{-3})
$X_{\text{HFO-H,P}}$	$X_{\text{HFO-H}}$ with bounded adsorption sites (ASM2d, ADM1) (g.m^{-3}) (kmol.m^{-3})
$X_{\text{HFO-H,P,old}}$	Old $X_{\text{HFO-H,P}}$ with bounded adsorption sites (ASM2d, ADM1) (g.m^{-3}) (kmol.m^{-3})
$X_{\text{HFO-L}}$	Hydrous ferric oxide with low number of active sites (ASM2d, ADM1) (g.m^{-3}) (kmol.m^{-3})
$X_{\text{HFO-L,P}}$	$X_{\text{HFO-L}}$ with bounded adsorption sites (ASM2d, ADM1) (g.m^{-3}) (kmol.m^{-3})
$X_{\text{HFO-L,P,old}}$	Old $X_{\text{HFO-L,P}}$ with bounded adsorption sites (ASM2d, ADM1) (g.m^{-3}) (kmol.m^{-3})
$X_{\text{HFO-old}}$	Inactive X_{HFO} (ASM2d, ADM1) (g.m^{-3}) (kmol.m^{-3})
X_{i}	Inert particulate organics (ASM2d, ADM1) (g COD.m^{-3}) (kg COD.m^{-3})
$X_{\text{KNH}_4\text{PO}_4}$	K-struvite (ASM2d, ADM1) (g.m^{-3}) (kmol.m^{-3})
X_{li}	Lipids (ADM1) (kg COD.m^{-3}) (g.m^{-3}) (kmol.m^{-3})
X_{MgCO_3}	Magnesite (ASM2d, ADM1) (g.m^{-3}) (kmol.m^{-3})
X_{MgHPO_4}	Newberyite (ASM2d, ADM1) (g.m^{-3}) (kmol.m^{-3})
$X_{\text{MgNH}_4\text{PO}_4}$	Struvite (ASM2d, ADM1) (g.m^{-3}) (kmol.m^{-3})
X_{PAO}	Phosphorus accumulating organisms (ASM2d, ADM1) (g COD.m^{-3}) (kg COD.m^{-3})
X_{PHA}	Polyhydroxyalkanoates (ASM2d, ADM1) (g COD.m^{-3}) (kg COD.m^{-3})
X_{PP}	Polyphosphates (ASM2, ADM1) (g.m^{-3}) (kmol.m^{-3})
X_{pr}	Proteins (ADM1) (kg COD.m^{-3})
X_{pro}	Propionate degraders (ADM1) (kg COD.m^{-3})
X_{SRB}	Sulfate-reducing bacteria (ADM1) (kg COD.m^{-3})
Z_{i}	Chemical species concentration of species i (algebraic variable of the physico-chemistry module) (kmol.m^{-3})

20 The objective of this paper is to report the effects that control/operational strategies may have on plant-wide
21 phosphorus (P) transformations in wastewater treatment plants (WWTP). The development of a new set of
22 biological (activated sludge, anaerobic digestion), physico-chemical (aqueous phase, precipitation, mass
23 transfer) process models and model interfaces (between water and sludge line) were required to describe the
24 required tri-phasic (gas, liquid, solid) compound transformations and the close interlinks between the P and
25 the sulfur (S) and iron (Fe) cycles. A modified version of the Benchmark Simulation Model No. 2 (BSM2)
26 (open loop) is used as test platform upon which three different operational alternatives (A_1 , A_2 , A_3) are
27 evaluated. Rigorous sensor and actuator models are also included in order to reproduce realistic control
28 actions. Model-based analysis shows that the combination of an ammonium (S_{NH_x}) and total suspended
29 solids (X_{TSS}) control strategy (A_1) better adapts the system to influent dynamics, improves phosphate (S_{PO_4})
30 accumulation by phosphorus accumulating organisms (X_{PAO}) (41 %), increases nitrification/denitrification
31 efficiency (18 %) and reduces aeration energy ($E_{aeration}$) (21 %). The addition of iron (X_{FeCl_3}) for chemical
32 P removal (A_2) promotes the formation of ferric oxides (X_{HFO-H} , X_{HFO-L}), phosphate adsorption ($X_{HFO-H,P}$,
33 $X_{HFO-L,P}$), co-precipitation ($X_{HFO-H,P,old}$, $X_{HFO-L,P,old}$) and consequently reduces the P levels in the effluent
34 (from 2.8 to 0.9 g P.m⁻³). This also has an impact on the sludge line, with hydrogen sulfide production
35 (G_{H_2S}) reduced (36 %) due to iron sulfide (X_{FeS}) precipitation. As a consequence, there is also a slightly
36 higher energy production ($E_{production}$) from biogas. Lastly, the inclusion of a stripping and crystallization
37 unit (A_3) for P recovery reduces the quantity of P in the anaerobic digester supernatant returning to the water
38 line and allows potential struvite ($X_{MgNH_4PO_4}$) recovery ranging from 69 to 227 kg.day⁻¹ depending on: (1)
39 airflow ($Q_{stripping}$); and, (2) magnesium ($Q_{Mg(OH)_2}$) addition. All the proposed alternatives are evaluated
40 from an environmental and economical point of view using appropriate performance indices. Finally, some
41 deficiencies and opportunities of the proposed approach when performing (plant-wide) wastewater treatment
42 modelling/engineering projects are discussed.

43 **KEYWORDS**

ACCEPTED MANUSCRIPT

44 benchmarking, control strategies, multiple mineral precipitation, physico-chemical modelling, nutrient
45 removal, struvite recovery

47 **RESEARCH HIGHLIGHTS**

- 48 • Development of a plant-wide model describing P (together with N, S, Fe), including pH prediction
- 49 • Operational strategies, such as aeration control and dosing of metals, have complex plant-wide
50 interactions
- 51 • Quantification of overall and individual N, P, S mass balances through the different process units
- 52 • Multi-criteria (economic/environmental) analysis of the evaluation results

70 The importance of plant-wide modelling has been emphasized by the chemical engineering community for a
71 long time and the wastewater industry is also realizing the benefits of this approach (**Skogestad, 2000;**
72 **Gernaey et al., 2014**). A wastewater treatment plant should be considered as an integrated process, where
73 primary/secondary clarifiers, activated sludge reactors, anaerobic digesters, thickener/flotation units,
74 dewatering systems, storage tanks, etc. are linked together and need to be operated and controlled not as
75 individual unit operations, but taking into account all the interactions amongst the processes (**Jeppsson et**
76 **al., 2013**). For this reason, during the last years wastewater engineering has promoted the development of
77 integrated modelling tools handling these issues (**Barker and Dold, 1997; Grau et al., 2007; Ekama, 2009;**
78 **Nopens et al., 2010; Gernaey et al., 2014**). Plant-wide models substantially increase the number of potential
79 operational strategies that can be simulated, and thereby enable the study of a new dimension of control
80 possibilities, such as studying the impact of activated sludge control strategies on the sludge line (**Jeppsson**
81 **et al., 2007**), the effect of primary sedimentation on biogas production (**Flores-Alsina et al., 2014a**) and the
82 handling of nitrogen-rich anaerobic digester supernatant (**Volcke et al., 2006a; Ruano et al., 2011; Flores-**
83 **Alsina et al., 2014a**).

84
85 Although being valuable tools, the state of the art is that these plant-wide models are limited to the
86 prediction of plant-wide organic carbon and nitrogen, and they are not properly taking into account the
87 transformation of phosphorus (P) and its close interlinks with the sulfur (S) and iron cycles (Fe), particularly in a
88 plant-wide context (**Batstone et al., 2015**). Phosphorus modelling is an essential requirement, particularly
89 considering its role in eutrophication of many catchments and its potential re-use as a fertilizer (**Verstraete**
90 **et al., 2009**). Therefore, this is an important issue for future model application and it will become of
91 paramount importance during the transition of wastewater treatment plants (WWTP) to water resource
92 recovery facilities (WRRFs), which will change the requirements for model-based analysis significantly for
93 wastewater engineering studies (**Vanrolleghem et al., 2014; Vanrolleghem and Vaneckhaute, 2014**).

95 The Activated Sludge Model No. 2d (ASM2d) specifically considers the role of phosphorus accumulating
96 organisms (PAO) in the water line (**Henze et al., 2000**). Similar P-related processes should be included in
97 the Anaerobic Digestion Model No. 1 (ADM1) (**Batstone et al., 2002**) as stated by Ikumi and co-workers
98 (**Ikumi et al., 2011, 2014**). Potential uptake of organics by PAO to form polyhydroxyalkanoates (PHA) with
99 the subsequent release of polyphosphates (PP) can also have an important effect on the anaerobic digestion
100 (AD) products (biogas, precipitates) (**Wang et al., 2016; Flores-Alsina et al., 2016**). Nevertheless the ASM
101 family (specifically the ASM2d for phosphorus) (**Henze et al., 2000**) and ADM1 (**Batstone et al., 2002**) are
102 inadequate to describe plant-wide P transformations. Part of this is because the physico-chemical
103 formulations in those models do not consider more complex phenomena in which P is involved. Indeed, P
104 trivalence gives a strong non-ideal behaviour, which requires amongst other factors, continuous ionic
105 strength tracking, extensive consideration of activities instead of molar concentrations and inclusion of
106 complexation/ion pairing processes (**Musvoto et al., 2000; Serralta et al., 2004; Solon et al., 2015; Flores-
107 Alsina et al., 2015; Lizarralde et al., 2015**). The latter is crucial to correctly describe chemical precipitation
108 and predict the fate of phosphorus compounds, and to properly predict nutrient cycling through the entire
109 plant (**Van Rensburg et al., 2003; Barat et al., 2011; Hauduc et al., 2015; Kazadi Mbamba et al., 2015a,
110 b**). There is also a general lack of consideration of biological and chemical transformation of Fe and S,
111 throughout both aerobic and anaerobic stages. Specifically, the sulfur cycle regulates Fe availability (and Fe
112 changes valency through oxidation/reduction) which then controls iron-phosphate complexing (**Gutierrez et
113 al., 2010; Flores-Alsina et al., 2016**). While biological and chemical complexation reactions of P have been
114 described in the AD unit, these have not generally been considered in plant-wide interactions with the Fe/S
115 cycles.

116
117 Model interfacing is also an important aspect to consider (**Batstone et al., 2015**) unless integrated plant-
118 wide models with a single set of state variables are used (**Barker and Dold, 1997; Grau et al., 2007;
119 Ekama et al., 2006; Barat et al., 2013**). Plant-wide modelling requires elemental mass balance verification
120 (**Hauduc et al., 2010**) and continuity checking for all the components included in the model (**Volcke et al.,
121 2006b; Zaher et al., 2007; Nopens et al., 2009**). Therefore, the quantities of C, N, P, Fe and S should be the

122 same before and after an interface (Flores-Alsina *et al.*, 2016). The main advantage of using an interface-
123 based approach with respect to other integrated methodologies is that the original model structure can be
124 used, and there is thus no need for state variable representation in all process units with the resulting
125 increased use of computational power, model complexity and adverse model stability characteristics (Grau
126 *et al.*, 2009).

127
128 The main objective of this paper is to present (for the first time): (1) an approach for mechanistic description
129 of all the main biological and physico-chemical processes required to predict organic P fluxes
130 simultaneously in both water and sludge lines in the WWTP under different operational modes; (2) an
131 analysis of the interactions between P, S and Fe on a plant-wide level; (3) a quantification of the compound
132 fluxes and pH variations in each unit and through the entire plant; and, (4) an evaluation of the different
133 operational/control strategies aimed at maximizing energy production, resource recovery and reduction of the
134 environmental impact and operating expenses measured as effluent quality (*EQI*) and operational cost indices
135 (*OCl*) (Copp, 2002; Nopens *et al.*, 2010). The paper details the development of the new plant-wide model by
136 presenting sequentially the different included sub-elements as well as the integration/interfacing aspects. The
137 capabilities/potential of the proposed approach is illustrated with several case studies. Lastly, opportunities and
138 limitations that arise from utilization of the new model are discussed as well.

139 **2. MODEL DESCRIPTION**

140 **2.1. Biological Models**

141 Sections 2.1.1 and 2.1.2 describe the additional processes and state variables included in the ADM1 and
142 ASM2d, respectively, in order to take into account biologically mediated phosphorus transformations
143 correctly. Additional modifications, with special emphasis to link the ADM and ASM with a physico-
144 chemical model, are described in Section 3 (Model integration). Model details, mass balances and continuity
145 verification can be found in the spreadsheet files provided within the Supplemental Information Section.

2.1.1. Anaerobic Digestion Model (ADM)

ACCEPTED MANUSCRIPT

The ADM1 version, implemented in the plant-wide context provided by the Benchmark Simulation Model No. 2 (BSM2) (Batstone *et al.*, 2002; Rosen *et al.*, 2006) is extended with P, S and Fe interactions (Flores-*Alsina et al.*, 2016). Phosphorus transformations account for kinetic decay of polyphosphates (X_{PP}) and potential uptake of volatile fatty acids (VFA) to produce polyhydroxyalkanoates (X_{PHA}) by phosphorus accumulating organisms (X_{PAO}) (Henze *et al.*, 2000; Harding *et al.*, 2011; Ikumi *et al.*, 2011; Wang *et al.*, 2016). Biological production of sulfides (S_{IS}) is described by means of sulfate-reducing bacteria (X_{SRB}) utilising hydrogen (autolithotrophically) as electron source (Batstone, 2006). Potential hydrogen sulfide (Z_{H_2S}) inhibition and stripping to the gas phase (G_{H_2S}) are considered (Fedorovich *et al.*, 2003; Pokorna-Krayzelova *et al.*, 2016). Finally, chemical iron (III) ($S_{Fe^{3+}}$) reduction to iron (II) ($S_{Fe^{2+}}$) is accounted for by using hydrogen (S_{H_2}) and sulfides (S_{IS}) as electron donors (Stumm and Morgan, 1996).

2.1.2. Activated Sludge Model (ASM)

A modified version of the Activated Sludge Model No. 2d (ASM2d) is selected to describe organic carbon, nitrogen and phosphorus transformations in the biological reactor (Henze *et al.*, 2000). In this implementation, biomass decay rates are electron-acceptor dependent (Siegrist *et al.*, 1999; Gernaey and Jørgensen, 2004). Potassium (S_K) and magnesium (S_{Mg}) are accounted for as new state variables and are included in the stoichiometry of formation and release of polyphosphates (X_{PP}). Another modification with respect to the original ASM2d is that total suspended solids is calculated from its constituents ($X_{TSS} = X_{VSS} + X_{ISS}$ are described separately) (Ekama and Wentzel, 2004; Ekama *et al.*, 2006) compared to the previous implementations wherein TSS is calculated as the sum of the assumed TSS content of each of the particulate state variables. This is mainly because the constituents of the inorganic suspended solids (X_{ISS}) are explicitly calculated as state variables with a contribution from polyphosphate (X_{PP}) in the activated sludge system. The model is also upgraded to describe the fate (oxidation/reduction reactions) of sulfur ($S_{SO_4^{2-}}$, S_{S_0} , S_{IS}) and iron ($S_{Fe^{3+}}$, $S_{Fe^{2+}}$) compounds in anaerobic, anoxic and aerobic conditions. Sulfate reduction is assumed to be biologically mediated by means of SRB (X_{SRB}) using two potential electron donors (S_A , S_F). Sulfide

171 (S_{IS}) and ($S_{\text{Fe}^{2+}}$) oxidation is described as a purely chemical reaction using different electron acceptors
ACCEPTED MANUSCRIPT
172 (S_{O_2} , S_{NO_x}) (Batstone, 2006; Batstone *et al.*, 2015; Gutierrez *et al.*, 2010; Stumm and Morgan, 1996).

173 **2.2. Physico-Chemical Models (PCM)**

174 **2.2.1. pH and ion speciation/pairing**

175 In this study a general aqueous phase chemistry model describing pH variation and ion speciation/pairing in
176 both ASM and ADM is used (Solon *et al.*, 2015; Flores-Alsina *et al.*, 2015). The model corrects for ionic
177 strength via the Davies' approach to consider chemical activities instead of molar concentrations,
178 performing all the calculations under non-ideal conditions. The general acid-base equilibria are formulated
179 as a set of implicit algebraic equations (IAEs) and solved separately at each time step of the ordinary
180 differential equation (ODE) solver using an extended multi-dimensional Newton-Raphson algorithm (Solon
181 *et al.*, 2015; Flores-Alsina *et al.*, 2015). Acid-base parameters and activity coefficients are corrected for
182 temperature effects. The species concentrations are expressed by a common nomenclature (Z_i) (Solon *et al.*,
183 2015) and participate in physico-chemical processes such as gas exchange and mineral precipitation (see
184 Sections 2.2.2 and 2.2.3).

185 **2.2.2. Multiple Mineral Precipitation (MMP)**

186 In this model, precipitation equations are described as a reversible process using the saturation index (SI) as
187 the chemical driving force. The SI represents the logarithm of the ratio between the product of the respective
188 activities of reactants that are each raised to the power of their respective stoichiometric coefficient, and the
189 solubility product constant (K_{sp}) (temperature corrected). If $SI < 0$ the liquid phase is assumed to be
190 undersaturated and a mineral might dissolve into the liquid phase, while if $SI > 0$ the liquid phase is assumed
191 to be supersaturated and mineral precipitation might occur (Stumm and Morgan, 1996). The precipitation
192 reaction rate depends on the kinetic rate coefficient, the concentration of the different species (Z_i), mineral
193 solid phase (X_i) and the order of the reaction (n) (Kazadi Mbamba *et al.*, 2015a, b). The proposed MMP
194 model includes the minerals: calcite (X_{CaCO_3}), aragonite ($X_{\text{CaCO}_{3a}}$), amorphous calcium phosphate
195 ($X_{\text{Ca}_3(\text{PO}_4)_2}$), hydroxylapatite ($X_{\text{Ca}_5(\text{PO}_4)_3(\text{OH})}$), octacalcium phosphate ($X_{\text{Ca}_8\text{H}_2(\text{PO}_4)_6}$), struvite ($X_{\text{MgNH}_4\text{PO}_4}$),

196 newberyite (X_{MgHPO_4}), magnesite (X_{MgCO_3}), k-struvite ($X_{\text{KNH}_4\text{PO}_4}$) and iron sulfide (X_{FeS}). A special
197 formulation is necessary to correctly describe precipitation of hydrous ferric oxides ($X_{\text{HFO-H}}$, $X_{\text{HFO-L}}$),
198 phosphate adsorption ($X_{\text{HFO-H,P}}$, $X_{\text{HFO-L,P}}$) and co-precipitation ($X_{\text{HFO-H,P,old}}$, $X_{\text{HFO-L,P,old}}$) (**Hauduc et al.,**
199 **2015**), since this is an adsorption rather than a precipitation reaction. Kinetic parameters were taken from
200 **Kazadi Mbamba et al. (2015a, b)** and **Hauduc et al. (2015)**.

201 **2.2.3. Gas-liquid transfer**

202 In open reactors, gas-liquid transfer is described as a function of the difference between the saturation
203 concentration and the actual concentration of the gas dissolved in the liquid and the contact area between the
204 gaseous and the aqueous phase (**Truskey et al., 2000**). The saturation concentration of the gas in the liquid
205 is given by Henry's law of dissolution, which states that the saturation concentration is equal to the product
206 of Henry's constant (K_H) multiplied by the partial pressure of the gas (P_i). The mass transfer rate constant
207 ($K_L a_i$) is calculated for each gaseous component ($i = Z_{\text{CO}_2}$, $Z_{\text{H}_2\text{S}}$, Z_{NH_3} and S_{N_2}). This $K_L a_i$ is calculated with
208 a proportionality factor relative to the reference compound oxygen ($K_L a_{\text{O}_2}$). The proportionality factor
209 depends on the relation between the diffusivity of the gas in the liquid (D_i) over the diffusivity of oxygen in
210 the liquid (D_{O_2}) (**Musvoto et al., 2000**). This does not apply for $K_L a_{\text{NH}_3}$ since NH_3 is a highly soluble gas
211 and thus its mass transfer is controlled by the transfer rate in the gas phase (**Lizarralde et al., 2015**). In
212 closed reactors, mass transfer between the liquid and the gas volume is described for selected gases ($i =$
213 Z_{CO_2} , $Z_{\text{H}_2\text{S}}$, Z_{NH_3} , S_{CH_4} and S_{H_2}) as described in **Rosen et al. (2006)**.

214 **2.3. Model Integration**

215 **2.3.1. ASM-PCM interface**

216 The default implementation of the ASM was adjusted in order to include the PCM (additional details can be
217 found in **Flores-Alsina et al. (2015)**). The main modifications are: (1) the use of inorganic carbon (S_{IC})
218 instead of alkalinity (S_{ALK}) as a state variable; (2) the inclusion of mass transfer equations for Z_{CO_2} , $Z_{\text{H}_2\text{S}}$,
219 Z_{NH_3} and S_{N_2} (**Batstone et al., 2012; Lizarralde et al., 2015**); (3) additional (and explicit) consideration of

multiple cations ($S_{\text{cat}}: S_{\text{K}}, S_{\text{Na}}, S_{\text{Ca}}, S_{\text{Mg}}$) and anions ($S_{\text{an}}: S_{\text{Cl}}$) which are tracked as soluble/reactive states; and, (4) chemical precipitation using metal hydroxides (X_{MeOH}) and metal phosphates (X_{MeP}) are omitted since the generalised kinetic precipitation model as described in **Kazadi Mbamba *et al.* (2015a, b)** and **Hauduc *et al.* (2015)** is used instead. Communication between the different models is straightforward. The outputs of the ASM at each integration step are used as inputs for the aqueous-phase module to estimate pH and ion speciation/pairing (works as a sub-routine) (see Section 2.2.1). The precipitation/stripping equations are formulated as ODEs and included in the overall mass balance.

2.3.2. ADM-PCM interface

The ADM is slightly modified to account for the updated physico-chemical model and new processes. The original pH solver proposed by **Rosen *et al.* (2006)** is substituted by the approach presented in **Solon *et al.* (2015)** and **Flores-Alsina *et al.* (2015)**. C, N, P, O and H fractions are taken from **de Gracia *et al.* (2006)**. Finally, the original ADM1 pools of undefined cations (S_{cat}) and anions (S_{an}) are substituted for specific compounds (see Section 2.3.1). The existing gas-liquid transfer equations are extended to include $Z_{\text{H}_2\text{S}}$ and Z_{NH_3} (**Rosen *et al.*, 2006**). Similarly as for the ASM-PCM interface, the pH and ion speciation/pairing model works as a sub-routine, while the multiple precipitation/stripping models are included within the system of ODEs in the ADM.

2.3.3. ASM-ADM-ASM interface

The interfaces between ASM-ADM-ASM are based on the continuity-based interfacing method (CBIM) described in **Volcke *et al.* (2006b)**, **Zaher *et al.* (2007)** and **Nopens *et al.* (2009)** to ensure elemental mass and charge conservation. The ASM-ADM-ASM interfaces consider: (1) (instantaneous) processes ($PROCESS_{\text{AS-AD}}/PROCESS_{\text{AD-AS}}$); and, (2) (state variable) conversions ($CONV_{\text{AS-AD}}/CONV_{\text{AD-AS}}$). On the one hand, the ASM-ADM interface instantaneous processes ($PROCESS_{\text{AS-AD}}$) involve (amongst others) instantaneous removal of COD demanding compounds (i.e. S_{O_2} and S_{NO_3}) and immediate decay of (heterotrophic/autotrophic) biomass. Conversions ($CONV_{\text{AS-AD}}$) require the transformation of soluble fermentable organics (S_{F}), acetate (S_{A}) and biodegradable particulate organics (X_{S}) into amino acids

245 (S_{aa})/sugars (S_{su})/fatty acids (S_{fa}) (soluble) and proteins (X_{pr})/lipids (X_{li})/carbohydrates (X_{ch}) (particulate),
246 respectively. On the other hand, the ADM-ASM interface assumes ($PROCESS_{AD-AS}$) that all compounds that
247 can be transferred into the gas phase (i.e. S_{H_2} and S_{CH_4}) are stripped, and also immediate decay of the AD
248 biomass takes place. $CONV_{AD-AS}$ turns all the biodegradable organic particulates (X_{pr} , X_{li} , X_{ch}), organic
249 solubles (S_{aa} , S_{fa} , S_{su}) and volatile fatty acids (S_{ac} , S_{pro} , S_{bu} , S_{va}) into X_S , S_F and S_A , respectively. There is
250 no variation of Fe and S before and after the interface. A comprehensive description with detailed
251 explanation of the involved processes, conversions and mass balance verification can be found in **Flores-**
252 **Alsina et al. (2016)**.

253 **2.4. Additional Elements**

254 **2.4.1. Influent generation/modelling principles**

255 The model blocks for: (1) flow rate generation (FLOW); (2) chemical oxygen demand (COD), N and P
256 generation (POLLUTANTS); (3) temperature profile generation (TEMPERATURE); and, (4) sewer
257 network and first flush effect (TRANSPORT) defined in **Gernaey et al. (2011)** are used to generate the
258 WWTP influent dynamics (12 months period of output data for the evaluation period with a 15 minutes
259 sampling interval). The resulting daily average influent mass flow rates are 8386 kg COD.d⁻¹, 1014 kg N.d⁻¹
260 and 197 kg P.d⁻¹ for COD, N and P, respectively (see **Figure SS1** in Supplemental Information for the
261 influent concentrations). The S:COD ratio is 0.003 kg S.kg COD⁻¹ (note that the S influent load is set to a
262 high value to have a noticeable effect in the AD). In addition, cation and anion profiles had to be added. The
263 resulting pH is close to neutrality (pH ~ 7). More information about the flow rate pollution dynamics and
264 how they are handled by the influent generator can be found in **Flores-Alsina et al. (2014b)**, **Martin and**
265 **Vanrolleghem (2014)** and **Snip et al. (2016)**.

266 **2.4.2. Ancillary processes and sensor/actuator models**

267 Primary clarification is described according to **Otterpohl and Freund (1992)**. The model is adjusted to
268 reflect the experiments carried out by **Wentzel et al. (2006)** where biodegradable/unbiodegradable
269 compounds show different settling velocities. The double exponential velocity function proposed by **Takács**

270 *et al.* (1991) using a 10-layer reactive configuration (Flores-Alsina *et al.*, 2012) is used as a fair
271 representation of the secondary settling process and reactions occurring in the settler. Several correlations
272 between sludge settleability parameters (such as stirred specific volume index, SSVI, and diluted sludge
273 volume index, DSVI) and the Takács settling parameters (maximum Vesilind settling velocity, v_0 , and
274 hindered zone settling parameter, r_h) (Gernaey *et al.*, 2014) have been used (Ekama *et al.*, 1997). A
275 reduction factor in the process kinetics is applied to the reactive secondary settler to obtain more realistic
276 results (Guerrero *et al.*, 2013). Flotation and dewatering units are described in Jeppsson *et al.* (2007).
277 Biological reactions in both units are included using the simplified approach described in Gernaey *et al.*
278 (2006). Stripping and crystallization units are described in Kazadi Mbamba *et al.* (2016). Response time,
279 delay and white noise are included in sensor/actuator models in order to avoid creating unrealistic control
280 applications (Rieger *et al.*, 2003).

281 2.4.3. Plant layout

282 The presented set of models is implemented in a plant layout that consists of a primary clarifier (PRIM), an
283 activated sludge unit (AS), a secondary settler (SEC2), a sludge thickener (THK/FLOT), an anaerobic
284 digester (AD), a storage tank (ST) and a dewatering unit (DW). The main modification with respect to the
285 original design (Nopens *et al.*, 2010) relies on the activated sludge (AS) configuration. An anaerobic section
286 (ANAER1, ANAER2) without oxygen (S_{O_2}) and nitrate (S_{NO_x}) is needed to promote anaerobic phosphorus
287 release and to provide the phosphorus accumulating organisms (X_{PAO}) with a competitive advantage over
288 other bacteria. Phosphorus release from the breakdown of polyphosphates (X_{PP}) provides the energy
289 required for anaerobic uptake of polyhydroxyalkanoates (X_{PHA}). Next, PAO grow using intracellular storage
290 products (i.e. X_{PHA}) as a substrate while taking up N and P as nutrients in the anoxic (ANOX1, ANOX2)
291 and aerobic (AER1, AER2, AER3) reactors with oxygen (S_{O_2}) or nitrate (S_{NO_3}) (with less efficiency) as
292 electron acceptors, respectively (see schematics in **Figure 1**). It is important to highlight that this
293 configuration does not represent an optimal design to remove P, because the biological P removal is
294 dependent on the N removal via the nitrate concentration recycled to the anaerobic reactor via the underflow
295 recycle (i.e. nitrates overflow may cause the anaerobic reactors to become anoxic). Nevertheless, it

296 exemplifies the retrofit of many (C, N removal) plants adapting their plant layout to satisfy new and stricter
297 effluent requirements (the authors do not presume that the given plant layout is the best configuration for
298 retrofit situations; a Modified UCT or a Johannesburg configuration may be more appropriate). Additional
299 details about the WWTP plant design and default operational conditions can be found in **Gernaey *et al.***
300 **(2014)** and in the software implementation (see Section 6).

301 **2.4.4. Evaluation criteria**

302 To assess the performance of combined N and P control strategies, an updated set of evaluation criteria are
303 necessary (**Jeppsson *et al.*, 2013**). The effluent quality index (*EQI*) (a weighted sum of effluent TSS, COD,
304 BOD, TKN and nitrate) is updated to include the additional P load (organic and inorganic). Additional P
305 upgrades have been necessary to include effluent violations (frequency and magnitude) and percentiles. The
306 cost of additional recycles (anoxic, anaerobic), aerators (CO₂ stripping) and chemicals (in case the user
307 wants to evaluate chemical P precipitation and recovery) are also added within the operational cost index
308 (*OCI*). A detailed description of the additional evaluation criteria is given in the Supplemental Information
309 Section.

310 **3. RESULTS AND DISCUSSION**

311 **3.1. Steady-State Simulations**

312 The steady-state simulations for the open loop configuration are summarized in **Figure 1** in terms of the
313 plant-wide overall mass balances and the individual ones for C, P, N, S, as well as for pH (plant-wide input
314 and output mass flows in bold). Around 49 % of the total incoming P load leaves the plant through the water
315 line (mainly as soluble phosphate, S_{PO_4}). The remaining P (51 %) goes to the sludge line (particulate). In the
316 AD unit, soluble S_{PO_4} is substantially increased as a result of biomass (X_B , X_A , X_{PAO}) and polyphosphates
317 (X_{PP}) decay. A fraction (78 %) of the incoming P to the digester precipitates ($X_{Ca_3(PO_4)_2}$, $X_{MgNH_4PO_4}$) or
318 becomes part of the organics (X_I , X_S). This will be disposed with the sludge. The remaining P is returned to
319 the water line as soluble phosphate (S_{PO_4}) (22 %). This increases the influent P load by almost 20 % (see
320 **Figure 1**). As a consequence of this extra load the overall plant performance (in terms of phosphorus

removal) for the open loop scenario is not good, giving effluent quality values ($TP = 4.6 \text{ g P.m}^{-3}$) well above the standards (assumed $TP_{\text{limit}} = 2.0 \text{ g P.m}^{-3}$).

Most of the nitrogen is depleted before reaching the sludge line (23 % remaining) through nitrification-denitrification, assimilation with the biomass and gas stripping. More specifically, around 32 % of the incoming N is converted to nitrogen gas (S_{N_2}) and 45 % leaves the plant in form of S_{NH_x} or S_{NO_x} . Simulated (N) effluent values ($TKN = 2.97 \text{ g N.m}^{-3}$ and $TN = 9.13 \text{ g N.m}^{-3}$) are well below the limits fixed by the BSM evaluation limit ($TKN_{\text{limit}} = 4 \text{ g N.m}^{-3}$ and $TN_{\text{limit}} = 15 \text{ g N.m}^{-3}$). The N load going to the sludge line (23 %) is basically associated with particulate organics (X_I, X_S) and biomass (X_B, X_A, X_{PAO}). Around 14 and 222 kg $N.day^{-1}$ are returned to the water line after flotation/thickening and dewatering, respectively, adding 23 % to the influent N load.

Sulfur arrives to the WWTP under study as sulfate (S_{SO_4}) and sulfides (S_{IS}) (S in the influent is set to a high value for demonstration purposes). In the anaerobic section of the activated sludge process there is a small reduction of S_{SO_4} to S_{IS} by SRB. In the anoxic/aerobic section most of the reduced S is re-oxidized to S_{SO_4} that becomes part of the effluent (93 %), a part is stripped to the atmosphere (5 %) and a small fraction of S_{SO_4} (2 %) is transported to the AD unit where it is converted to hydrogen sulfide gas (G_{H_2S}) (65 %) and dissolved sulfides (S_{IS}) (25 %) with a concentration of 32 g S.m^{-3} (biogas composition by volume: $G_{CH_4} = 62.00 \%$, $G_{CO_2} = 37.46 \%$, $G_{H_2S} = 0.54 \%$). A small fraction of sulfate remains unconverted (S_{SO_4}) (10 %). The soluble S fractions are returned to the water line and are re-oxidized to sulfate in the activated sludge reactor. Compared to the N and P streams, the resulting increase in the influent S load is not very high (increase of 2 %).

Influent pH is close to neutrality ($pH = 7.06$). In this particular case, at the end of the water line pH is increased mainly due to carbon dioxide (Z_{CO_2}) stripping. Nevertheless, in other cases for systems with low buffer capacity, the loss of alkalinity via nitrification might decrease the pH far more strongly (**Henze *et al.***,

2008). The almost anaerobic conditions in the first units of the sludge line (secondary settler and thickener/flotation units) promote: (1) fermentation of organic soluble substrate (S_F) to acetate (S_A); and, (2) decay of X_{PP} and subsequent release of S_{IP} . As a consequence, there is a decrease of pH. In the AD, pH is slightly reduced again as a result of multiple mineral precipitation. In the dewatering unit, pH is raised again due to Z_{CO_2} stripping. There is no effect on the influent entering the primary clarifier. Similar observations about pH behaviour through the different plant units are reported in **Lizarralde et al. (2015)** and **Kazadi Mbamba et al. (2016)**.

3.2. Dynamic Simulations

All dynamic simulations (609 days) are preceded by steady-state simulations (300 days) but only the data generated during the final 364 days are used for plant performance evaluation. Default (open loop) operational conditions (**Gernaey and Jørgensen, 2004**) represent the baseline configuration (A_0) upon which the different operational/control/recovery strategies will be implemented, simulated and evaluated (see **Table 1**). **Figure 2** shows dynamic profiles for selected influent (**Figures 2a, b**), effluent (**Figures 2d, e**) and operational (**Figures 2c, f, g, h**) variables.

3.2.1. Control strategy (A_1): Cascade ammonium + wastage controller

The first alternative control strategy (A_1) is based on a cascade PI ammonium (S_{NH_x}) controller that manipulates the (S_{O_2}) set-point in AER2 (and also the airflow in AER1 and AER3 by a factor of 2.0 and 0.5, respectively) (**Figure 3a**). The S_{O_2} concentration in AER2 is controlled by manipulating the air supply rate. The second controller regulates the total suspended solids (X_{TSS}) in AER3 by manipulating the wastage flow (Q_w) (**Vanrolleghem et al., 2010**). The set-point changes (set-point = $3000 \text{ gTSS.m}^{-3} > 15^\circ\text{C}$ / $4000 \text{ gTSS.m}^{-3} < 15^\circ\text{C}$) are made according to temperature (T) in order to set a longer SRT to maintain the nitrification capacity during the winter period (**Figure 3b**). Additional details about the simulated control strategies can be found in **Table 1**. The S_{O_2} and T sensor are assumed to be close to ideal with a response time of 1 minute in order to prevent unrealistic control applications. On the other hand, the S_{NH_x} sensor has a time delay of 10 minutes, with zero mean white noise (standard deviation of 0.5 g N.m^{-3}) (**Rieger et al.,**

2003). The aeration system and the wastage pumping system are defined with significant dynamics assuming a response time of 4 minutes. **Table 2** summarizes the values for the different evaluation criteria. The implementation of these controllers improves S_{PO_4} accumulation by X_{PAO} and increases nitrification/denitrification efficiency. This is mainly due to a better aeration strategy in the biological reactors. As a side effect, operational cost (OCI) is reduced and there is a substantial reduction of the energy consumed (see $E_{aeration}$ values in **Table 2**). As a further consequence, effluent quality values (N_{total} , P_{total} , E_{QI}) are improved. Indeed, the open loop aeration system is highly inefficient (not sufficient during daytime and excessive at night) (see **Figure 2c**). Summer/winter wasting schemes cause variations in the quantity of sludge arriving to the AD and therefore changes in the biogas production. This is translated into different potential energy recovery efficiencies (see $E_{production}$ values in **Table 2**).

3.2.2. Control strategy (A_2): Fe chemical precipitation in the AS section

The second alternative (A_2) involves the addition of iron (as X_{FeCl_3} , the model assumes a liquid solution of X_{FeCl_3}) in the AS section in addition to A_1 (see **Table 1**). The S_{PO_4} concentration in AER3 is controlled by manipulating the metal flow rate (Q_{FeCl_3}) (**Figure 4a**). Additional details about the simulated control strategies can be found in **Table 1**. The S_{PO_4} and S_{NH_x} sensors have similar characteristics (10 minutes delay and zero mean white noise with a standard deviation of $0.5 \text{ g P or N.m}^{-3}$). Response time for Q_{FeCl_3} is also 10 minutes (avoiding unrealistic control actions).

Results reported in **Table 2** show a reduction in P_{inorg} , time in violation (TIV) P_{total} as well as the E_{QI} due to chemical P precipitation (see **Figures 2e** and **4a**, respectively). On the other hand, there is an increase in sludge production (SP_{total}) and the OCI as a trade-off. The aeration energy ($E_{aeration}$) also slightly increase from scenario A_1 to A_2 mainly due to reduced PAO activity brought about by chemical phosphorus removal; less organics are taken up by in the anaerobic part of the activated sludge unit in scenario A_2 and, as a consequence, more organics need to be oxidized in the aerobic part. It is important to highlight the additional beneficial effect of X_{FeCl_3} addition in the sludge line. Indeed, under anaerobic conditions hydrous

ferric oxides ($X_{\text{HFO-H}}$, $X_{\text{HFO-L}}$) are chemically reduced to Fe (II) ($S_{\text{Fe}^{2+}}$) using hydrogen (S_{H_2}) and/or sulfides (S_{IS}) as electron donors. Also, iron phosphates ($X_{\text{HFO-H,P}}$, $X_{\text{HFO-L,P}}$) formed in the activated sludge process water line might re-dissolve under anaerobic conditions in the digesters to precipitate with sulfide (X_{FeS}). This is due to the much lower solubility of iron sulfide as compared to iron phosphate (Stumm and Morgan, 1996). The control strategy reduces undesirable inhibition/odour/corrosion problems, as well as risks for human health, as indicated by the higher G_{CH_4} and lower $G_{\text{H}_2\text{S}}$ values compared to (A_1) (see Figures 2h and 4b, respectively). Similar conclusions were reached by the experimental campaigns/measurements run by Mamais *et al.* (1994), Ge *et al.* (2013) and Zhang *et al.* (2013).

It is important to highlight that the addition of Fe substantially changes the whole P and S cycle through the entire plant while N fluxes are barely affected. The fraction of P sent to the sludge line is increased from 51 to 67 % (94 to 127 kg P.day⁻¹) (mainly as $X_{\text{HFO-H,P}}$, $X_{\text{HFO-L,P}}$, $X_{\text{HFO-H,P,old}}$, $X_{\text{HFO-L,P,old}}$) (see Figure SS2 in Supplemental Information). This Fe addition reduces the quantity of $X_{\text{Ca}_3(\text{PO}_4)_2}$ and $X_{\text{MgNH}_4\text{PO}_4}$ formed in the AD which, from a practical point of view, leads to less problems with their deposition in the pipes. Similar findings are also found in the following studies: Luedecke *et al.* (1989); Doyle and Parsons (2002) and Mamais *et al.* (1994). When it comes to S, there is a substantial reduction of the quantity of $Z_{\text{H}_2\text{S}}$ in the AD due to the preferential binding with Fe (from 5100 to 4400 ppm). As a result, there is a lower quantity of H_2S in the gas phase and therefore the quantity of S leaving the plant via sludge disposal (as precipitate X_{FeS}) increases. There is a slight decrease of pH due to the increase of the contra-ion Cl^- added as part of the iron precipitation.

3.2.3. Control strategy (A_3): Potential P recovery as struvite in the digester supernatant

The last alternative implies a modification of the original plant layout by adding a stripping unit (STRIP) for pH increase, a crystallizer (CRYST) to facilitate struvite recovery, a magnesium hydroxide dosage tank ($X_{\text{Mg}(\text{OH})_2}$) and a dewatering unit (DEW2) for potential P recovery (Kazadi Mbamba *et al.*, 2016). The assumed hydraulic retention times (HRT) of the STRIP and CRYST units are approximately 2 h and 18 h,

423 respectively (Tchobanoglous *et al.*, 2003). **Figure SS3** (in Supplemental Information) shows the effect of
 424 the extra units on the total P fluxes. Simulation results indicate that the quantity of returning N and P from
 425 the AD supernatant is reduced from 221 to 201 kg N.day⁻¹ and 30 to 1.3 kg P.day⁻¹, respectively (as a result
 426 of recovering P as $X_{MgNH_4PO_4}$). The latter leads to a reduction of the nutrient load to be treated in the
 427 biological reactor and decreases the quantity of P lost in the effluent (from 96 to 60 kg P.day⁻¹). When this is
 428 translated to evaluation indices (**Table 2**), a substantial reduction in the effluent related criteria (N_{total} ,
 429 P_{total} , EQI) can be seen. The OCI is lower compared to A_2 due to: (1) the lower price of magnesium
 430 hydroxide ($X_{Mg(OH)_2}$) compared to iron chloride (X_{FeCl_3}); and, (2) the potential economic benefit resulting
 431 from selling struvite ($X_{MgNH_4PO_4}$).

432
 433 Additional simulations show that these values can be modified by changing the airflow ($Q_{stripping}$) and the
 434 chemical dosage ($Q_{Mg(OH)_2}$) in the stripping unit. At high airflows ($Q_{stripping}$) the quantity of Z_{CO_2} stripped
 435 increases and consequently the pH (CO_2 has acidifying behaviour) (**Figures 5a, h**). The latter favours
 436 struvite ($X_{MgNH_4PO_4}$) precipitation (**Figures 5b, g**). A higher quantity of Mg ($Q_{Mg(OH)_2}$) also drives the pH
 437 higher (**Figures 5a, f**). These results show that $X_{MgNH_4PO_4}$ precipitation is mainly limited by $Z_{Mg^{2+}}$ rather
 438 than $Z_{NH_4^+}$ and $Z_{PO_4^{3-}}$. This explains the substantial increase of $X_{MgNH_4PO_4}$ when the quantity of Mg is higher
 439 (note that an overdose of magnesium is also not beneficial due to possible precipitation of dolomite, etc.).
 440 The latter has an effect on P in the AD supernatant (**Figure 5e**) and consequently the EQI (**Figure 5c**). High
 441 $Q_{Mg(OH)_2}$ decreases the OCI since the struvite ($X_{MgNH_4PO_4}$) is accounted for as a potential benefit (**Figure**
 442 **5d**). Above the P/Mg stoichiometric ratios, additional Mg is just increasing the cost without further benefit,
 443 $Q_{Mg(OH)_2} > 40$ kg Mg.day⁻¹. **Figures 5e, f, g** and **h** show the dynamic profiles of pH at different
 444 $Q_{stripping}/Q_{Mg(OH)_2}$. One might notice the effect that the X_{TSS} controller has on the quantity of sludge
 445 leaving the AD as a result of changing the TSS set-point in AER3.

3.2.4. Environmental/economic evaluation summary

ACCEPTED MANUSCRIPT

In all cases, the proposed alternatives (A_1 , A_2 , A_3) result in substantial improvements with respect to the open loop default configuration (A_0). The implementation of a better aeration strategy and time-varying sludge wasting scheme (A_1) results in a favourable alternative. Simulation results show that this option leads to larger N and P effluent reductions, but also a more cost-effective way to operate the plant. Both A_2 and A_3 substantially reduce the quantity of effluent P. The main difference between the two relies on that A_3 implies a major modification of the plant layout. Capital expenditures of the CRYST, STRIP, blowers, civil, electrical and piping works should be included in order to make a more complete assessment. In contrast, alternative A_2 can be arranged easily with an extra dosing tank. Even though the potential benefit that comes from struvite ($S_{\text{recovered}}$) recovery is very uncertain and these results should be taken with care (Shu *et al.*, 2006; Vaneckhaute *et al.*, 2015), the cost for each kg N and P removed is much higher for A_2 (see N_{removed}/OCI and P_{removed}/OCI values in Table 2). The latter means that the cost is dramatically lower for A_3 and payback time for the new installation should be short. It is important to highlight that a thorough economic study is not carried out in this paper since it is not within the scope of the study.

4. CHALLENGES AND LIMITATIONS OF THE PROPOSED APPROACH

The model results presented in this paper demonstrate the effects that different operational modes might have on the physico-chemical and biological transformations of P in a WRRF. The observations noted above also suggest the importance of linking the P with the S and Fe cycles since this paper identifies that potential control strategies not only address the primary goal, but have an effect that is cycled throughout the process (see Figures 1, SS2). This is critical to enable the development, testing and evaluation of phosphorus control/recovery strategies in the context of water resource recovery facilities (Jeppsson *et al.*, 2013). In the following section, we discuss the applicability of the model assumptions made to describe P, S and Fe interactions, the suitability of the number of considered processes and some practical implications for plant-wide modelling/development of resource recovery strategies.

4.1. Selection of the Relevant Process and Interpretation of the Results

ACCEPTED MANUSCRIPT

The model presented in this paper accounts for some of the most important factors affecting the P, S and Fe cycles in a wastewater treatment facility (**Batstone et al., 2015**). Additional processes may be added to consider novel control strategies. For example, sulfide can be directly controlled in the digester through microaeration, which converts sulfide to elemental sulfur (**Krayzelova et al., 2015**). The approach taken in this paper in describing sulfide oxidation to elemental sulfur in the anaerobic zone of the activated sludge process is directly applicable to this problem.

When it comes to P recovery, important assumptions were made in order to run the third alternative (A_3). For example, calcium precipitation is not assumed in the crystallizer. This is due to the low amounts of calcium in this scenario, and because calcium generally complexes with carbonate (**Kazadi Mbamba et al., 2015a**). In high-calcium (hard) waters, it may become critical. Another important factor is that ideal solids separation in the crystallizer is assumed. This will depend on the specific implementation of the crystallizer and crystal recovery. Precipitate dissolution (and particularly Mg dissolution) is currently simplified. The latter may have an important effect on the overall process performance (**Romero-Güiza et al., 2015**). In the water line, competition between PAO and Glycogen Accumulating Organisms (GAO) (**Lopez-Vazquez et al., 2007, 2009; Oehmen et al., 2010**) is not accounted for. This may have a strong influence on the overall biological P removal. S and Fe oxidation processes have been modelled chemically, but there are numerous studies demonstrating that these processes are also biologically mediated (**Xu et al., 2013**). In any case, the oxidation processes goes to completion. This may have limited impact on the overall process, due to the ubiquitous capability of sulfur oxidation/reduction capability in heterotrophic organisms.

The alternating aerated/non-aerated periods might promote the formation of nitrous oxide gases (**Ni et al., 2014; Ni and Yuan, 2015**). When evaluating the suitability of different control/operational strategies, this factor is not included in the study, and if it was, it might partly change the overall discussion of the results (**Flores-Alsina et al., 2014a; Sweetapple et al., 2015; Mannina et al., 2016**). Closely related to that, it is important to point out that aeration energy could be better estimated with a more detailed piping/distribution

497 model (**Beltrán et al., 2011**). In addition, the aeration model could be further improved using a detailed
498 mass transfer model which might change the quantity of stripped gas (that might be overestimated with the
499 current model) (**Lizarralde et al., 2015**). All these options, including evaluating the impact of influent flow
500 equalization basins, are identified as promising research avenues that will be further studied in the near
501 future (**Jeppsson et al., 2013**). The latter could be combined with proper electricity tariff models (**Aymerich
502 et al., 2015**) and dramatically change the way how energy must be optimized. In this case study relative
503 costs have been used (**Jeppsson et al., 2007**) due to the volatility of the prices (chemicals, electricity, sludge
504 disposal, ...). Proper cost estimates and variations (uncertainty ranges) will provide customized solutions for
505 a particular case.

506 **4.2. General Applicability of the Presented Model**

507 Even though the shown numeric results are case-specific, the presented tools are generally applicable, and
508 an earlier version has been successfully applied to a real plant (**Kazadi Mbamba et al., 2016**). The influent
509 characteristics (**Gernaey et al., 2011**) can be scaled to different situations (**Flores-Alsina et al., 2014b; Snip
510 et al., 2016; Kazadi Mbamba et al., 2016**). The original BSM2 (only carbon and nitrogen) plant has been
511 adapted to simulate the dynamics of some Swedish plants (**Arnell et al., 2013**). The ASM2d and ADM1
512 (separately) have been applied to multiple case studies successfully describing plant dynamics (**Gernaey et
513 al., 2004; Batstone et al., 2015**). The P principles upon which the new AD model is constructed are
514 experimentally validated in different studies (**Ikumi et al., 2011; Wang et al., 2016**). The same applies to
515 the S module in both AS (**Gutierrez et al., 2010**) and AD (**Batstone et al., 2006; Barrera et al., 2015**)
516 models. As stated above, expansion to consider cases such as microaeration in anaerobic digesters can be
517 done through direct adaptation of the approach taken in the activated sludge process.

518
519 The model may also be applied to integrated urban water systems, wherein, chemicals added/present in the
520 sewer network or during drinking water production may have an impact on the downstream wastewater
521 treatment processes (particularly for systems where there is no primary sedimentation) (**Pikaar et al., 2014;
522 Nielsen et al., 2005; Ge et al., 2012**).

4.3. Optimization tool for resource recovery

The described approach has strong potential for optimizing resource recovery (i.e. biogas and phosphorus recovery) in a plant-wide context, and possibly also in the larger sewage catchment. For example, the potential energy/financial benefits of an improved biogas production can be balanced with the addition of selected chemicals (Flores-Alsina *et al.*, 2016) or substrates for co-digestion (Arnell *et al.*, 2016). Another potential option is P recovery (Vaneckhaute, 2015). Results presented in Section 3.2.3 show that the total quantity of recovered P is rather small (31.8 kg P.d⁻¹/196.6 kg P.d⁻¹). This is mainly due to the different P losses/transformations through the different units in the plant. Different operational conditions (Marti *et al.*, 2008, 2010; Latif *et al.*, 2015) could reduce the quantity of P lost in the effluent, could minimize uncontrolled phosphorus precipitation in the anaerobic digester and enhance phosphorus recovery in the crystallizer. In a similar way, smarter dosing strategies (similarly to A₂) could be evaluated in order to reduce the use of chemicals and to adapt to changes in the P loads due to operational changes (summer/winter). Airflow in the stripping unit could be adjusted in order to reach a desired pH (feedback controller).

5. CONCLUSIONS

The main findings of this study are summarized in the following points:

- 1) A plant-wide model describing the main P transformations and the close interactions with the S and Fe cycles in wastewater treatment systems is presented;
- 2) Operational conditions have a strong effect on the fate of P compounds: accumulation by X_{PAO} , adsorption into Fe ($X_{\text{HFO-H,P}}$, $X_{\text{HFO-L,P}}$) and co-precipitation with different metals ($X_{\text{HFO-H,P,old}}$, $X_{\text{HFO-L,P,old}}$, $X_{\text{Ca}_3(\text{PO}_4)_2}$, $X_{\text{MgNH}_4\text{PO}_4}$);
- 3) Overall and individual mass balances quantify the distribution of P (as well as N and Fe) in both water and sludge line;
- 4) The set of models presented in this study makes up a useful engineering tool to aid decision makers/wastewater engineers when upgrading/improving the sustainability and efficiency of wastewater treatment systems (e.g. reduce consumption and increase recovery).

6. SOFTWARE AVAILABILITY

ACCEPTED MANUSCRIPT

The MATLAB/SIMULINK code of the models presented in this paper is available upon request, including the implementation of the physico-chemical and biological modelling framework in BSM2. Using this code, interested readers will be able to reproduce the results summarized in this study. To express interest, please contact Dr. Ulf Jeppsson (ulf.jeppsson@iea.lth.se) at Lund University (Sweden), Prof. Krist V. Gernaey (kvg@kt.dtu.dk) or Dr. Xavier Flores-Alsina (xfa@kt.dtu.dk) at the Technical University of Denmark (Denmark) or Dr. Damien Batstone (damienb@awmc.uq.edu.au) at The University of Queensland (Australia).

7. ACKNOWLEDGEMENTS

Ms Solon and Dr Flores-Alsina acknowledge the Marie Curie Program of the EU 7th Framework Programme FP7/2007-2013 under REA agreement 289193 (SANITAS) and 329349 (PROTEUS), respectively. Dr Flores-Alsina gratefully acknowledges the financial support of the collaborative international consortium WATERJPI2015 WATINTECH of the Water Challenges for a Changing World Joint Programming Initiative (Water JPI) 2015 call. Parts of this research were developed during the research stay of Dr Flores-Alsina at the Department of Civil Engineering at the University of Cape Town (South Africa) and at the Advanced Water Management Centre at The University of Queensland (Australia) and also developed during the short term scientific COST mission (STSM, COST Water2020) of Ms Solon at the Biosystems Control research unit at the Department of Biosystems Engineering at Ghent University (Belgium). The research was supported financially by The University of Queensland through the UQ International Scholarships (UQI). Peter Vanrolleghem holds the Canada Research Chair in Water Quality Modelling. Dr. Stephan Tait at the Advanced Water Management Centre, The University of Queensland (Australia), is acknowledged for his valuable contributions on the discussions during the model development. The International Water Association (IWA) is also acknowledged for their promotion of this collaboration through their sponsorship of the IWA Task Group on Generalized Physicochemical Modelling Framework (PCM). A concise version of this paper was presented at Watermatex 2015 (Gold Coast, Australia, June, 2015).

8. REFERENCES

- 575
576 Arnell, M., Astals, S., Åmand, L., Batstone, D.J., Jensen, P.D. & Jeppsson, U. (2016). Modelling anaerobic
577 co-digestion in Benchmark Simulation Model No. 2: Parameter estimation, substrate characterisation
578 and plant-wide integration. *Water Research*, 98, 138-146.
- 579 Arnell, M., Sehlen, R. & Jeppsson, U. (2013). Practical use of wastewater treatment modelling and
580 simulation as a decision support tool for plant operators—case study on aeration control at Linköping
581 wastewater treatment plant. In: *Proceedings of the 13th Nordic Wastewater Conference*, Malmö,
582 Sweden, 8-10 October 2013.
- 583 Aymerich, I., Rieger, L., Sobhani, R., Rosso, D. & Corominas, L. (2015). The difference between energy
584 consumption and energy cost: Modelling energy tariff structures for water resource recovery
585 facilities. *Water Research*, 81, 113-123.
- 586 Barat, R., Montoya, T., Seco, A. & Ferrer, J. (2011). Modelling biological and chemically induced
587 precipitation of calcium phosphate in enhanced biological phosphorus removal systems. *Water
588 Research*, 45(12), 3744-3752.
- 589 Barat, R., Serralta, J., Ruano, V., Jimenez, E., Ribes, J., Seco, A. & Ferrer, J. (2013). Biological Nutrient
590 Removal no 2 (BNRM2): a general model for wastewater treatment plants. *Water Science &
591 Technology*, 67(7), 1481-1489.
- 592 Barker, P.S. & Dold, P.L. (1997). General model for biological nutrient removal activated-sludge systems:
593 model presentation. *Water Environment Research*, 69(5), 969-984.
- 594 Barrera, E.L., Spanjers, H., Solon, K., Amerlinck, Y., Nopens, I. & Dewulf, J. (2015). Modeling the
595 anaerobic digestion of cane-molasses vinasse: Extension of the Anaerobic Digestion Model No. 1
596 (ADM1) with sulfate reduction for a very high strength and sulfate rich wastewater. *Water Research*,
597 71, 42-54.
- 598 Batstone, D.J. (2006). Mathematical modelling of anaerobic reactors treating domestic wastewater: Rational
599 criteria for model use. *Reviews in Environmental Science and Biotechnology*, 5, 57-71.

- 600 Batstone, D.J., Keller, J., Angelidaki, I., Kalyuzhnyi, S.V., Pavlostathis, S.G., Rozzi, A., Sanders, W.T.M.,
ACCEPTED MANUSCRIPT
601 Siegrist, H. & Vavilin V.A. (2002). Anaerobic Digestion Model No. 1. IWA Scientific and Technical
602 Report No. 13. London, UK: IWA Publishing.
- 603 Batstone, D.J., Puyol, D., Flores-Alsina, X. & Rodriguez, J. (2015). Mathematical modelling of anaerobic
604 digestion processes: Applications and future needs. *Reviews on Environmental Science and*
605 *Biotechnology*, 14(4), 595-613.
- 606 Beltrán, S., Logrono, C., Maiza, M. & Ayesa, E. (2011). Model based optimization of aeration system in
607 WWTP. In: *Proceedings of Watermatex2011, San Sebastian, Spain, 20-22 June 2011*.
- 608 Copp, J.B. (ed.) (2002). *The COST Simulation Benchmark – Description and Simulator Manual*. ISBN 92-
609 894-1658-0, Office for Official Publications of the European Communities, Luxembourg.
- 610 de Gracia, M., Sancho, L., García-Heras, J.L., Vanrolleghem, P. & Ayesa, E. (2006). Mass and charge
611 conservation check in dynamic models: Application to the new ADM1 model. *Water Science &*
612 *Technology*, 53(1), 225-240.
- 613 Doyle, J.D. & Parsons, S.A. (2002). Struvite formation, control and recovery. *Water Research*, 36(16),
614 3925-3940.
- 615 Ekama, G.A. (2009). Using bioprocess stoichiometry to build a plant-wide mass balance based steady-state
616 WWTP model. *Water Research*, 43(8), 2101-2120.
- 617 Ekama, G.A., Barnard, J.L., Gunthert, F.W., Krebs, P., McCorquodale, J.A., Parker, D.S. & Wahlberg, E.J.
618 (1997). *Secondary settling tanks: Theory, modelling, design and operation*. IWA Scientific and
619 *Technical Report No. 6*. London, UK: IWA Publishing.
- 620 Ekama, G.A. & Wentzel, M.C. (2004). A predictive model for the reactor inorganic suspended solids
621 concentration in activated sludge systems. *Water Research*, 38(8), 4093-4106.
- 622 Ekama, G.A., Wentzel, M.C. & Sötemann, S.W. (2006). Tracking the inorganic suspended solids through
623 biological treatment units of wastewater treatment plants. *Water Research*, 40(19), 3587-3595.
- 624 Fedorovich, V., Lens, P. & Kalyuzhnyi, S. (2003). Extension of Anaerobic Digestion Model No. 1 with
625 processes of sulfate reduction. *Applied Biochemistry and Biotechnology*, 109, 33-45.

- 626 Flores-Alsina, X., Arnell, M., Amerlinck, Y., Corominas, L., Gernaey, K.V., Guo, L., Lindblom, E.,
ACCEPTED MANUSCRIPT
627 Nopens, I., Porro, J., Shaw, A., Snip, L., Vanrolleghem, P.A. & Jeppsson, U. (2014a). Balancing
628 effluent quality, economical cost and greenhouse gas emissions during the evaluation of plant-wide
629 wastewater treatment plant control strategies. *Science of the Total Environment*, 466-467, 616-624.
- 630 Flores-Alsina, X., Gernaey, K.V. & Jeppsson, U. (2012). Benchmarking biological nutrient removal in
631 wastewater treatment plants: influence of mathematical model assumptions. *Water Science &
632 Technology*, 65(8), 1496-1505.
- 633 Flores-Alsina, X., Kazadi Mbama, C., Solon, K., Vrecko, D., Tait, S., Batstone, D., Jeppsson U. & Gernaey
634 K.V. (2015). A plant-wide aqueous phase chemistry module describing pH variations and ion
635 speciation/pairing in wastewater treatment models. *Water Research*, 85, 255-265.
- 636 Flores-Alsina, X., Saagi, R., Lindblom, E., Thirsing, C., Thornberg, D., Gernaey, K.V. & Jeppsson, U.
637 (2014b). Calibration and validation of a phenomenological influent pollutant disturbance scenario
638 generator using full-scale data. *Water Research*, 51, 172-185.
- 639 Flores-Alsina, X., Solon, K., Kazadi Mbamba, C., Tait, S., Jeppsson, U., Gernaey, K.V. & Batstone, D.J.
640 (2016). Modelling phosphorus, sulphur and iron interactions during the dynamic simulation of
641 anaerobic digestion processes. *Water Research*, 95, 370-382.
- 642 Ge, H., Zhang, L., Batstone, D.J., Keller, J. & Yuan, Z. (2013). Impact of iron salt dosage to sewers on
643 downstream anaerobic sludge digesters: Sulfide control and methane production. *Journal of
644 Environmental Engineering*, 139, 594-601.
- 645 Gernaey, K.V., Flores-Alsina, X., Rosen, C., Benedetti, L. & Jeppsson, U. (2011). Dynamic influent
646 pollutant disturbance scenario generation using a phenomenological modelling approach.
647 *Environmental Modelling & Software*, 26(11), 1255-1267.
- 648 Gernaey, K.V., Jeppsson, U., Batstone, D.J. & Ingildsen, P. (2006). Impact of reactive settler models on
649 simulated WWTP performance. *Water Science & Technology*, 53(1), 159-167.
- 650 Gernaey, K.V., Jeppsson, U., Vanrolleghem, P.A. & Copp, J.B. (2014). Benchmarking of control strategies
651 for wastewater treatment plants. IWA Scientific and Technical Report No. 23. London, UK: IWA
652 Publishing.

- 653 Gernaey, K.V. & Jørgensen, S.B. (2004). Benchmarking combined biological phosphorus and nitrogen
654 removal wastewater treatment processes. *Control Engineering Practice*, 12(3), 357-373.
- 655 Grau, P., Copp, J., Vanrolleghem, P.A., Takács, I. & Ayesa, E. (2009). A comparative analysis of different
656 approaches for integrated WWTP modelling. *Water Science & Technology*, 59(1), 141-147.
- 657 Grau, P., de Gracia, M., Vanrolleghem, P.A. & Ayesa, E. (2007). A new plant-wide modelling methodology
658 for WWTPs. *Water Research*, 41(19), 4357-4372.
- 659 Gutierrez, O., Park, D., Sharma, K.R. & Yuan, Z. (2010). Iron salts dosage for sulfide control in sewers
660 induces chemical phosphorus removal during wastewater treatment. *Water Research*, 44(11), 3467-
661 3475.
- 662 Guerrero, J., Flores-Alsina, X., Guisasola, A., Baeza, J.A. & Gernaey, K.V. (2013). Effect of nitrite, limited
663 reactive settler and plant design configuration on the predicted performance of a simultaneous C/N/P
664 removal WWTP. *Bioresource Technology*, 136, 680-688.
- 665 Harding, T.H., Ikumi, D.S. & Ekama, G.A. (2011). Incorporating phosphorus into plant wide wastewater
666 treatment plant modelling anaerobic digestion. In: *Proceedings of Watermatex2011*, San Sebastian,
667 Spain, 20-22 June 2011.
- 668 Hauduc, H., Rieger, L., Takács, I., Héduit, A., Vanrolleghem, P.A. & Gillot, S. (2010). A systematic
669 approach for model verification: Application on seven published activated sludge models. *Water
670 Science and Technology*, 61(4), 825-839.
- 671 Hauduc, H., Takács, I., Smith, S., Szabo, A., Murthy, S., Daigger, G. T. & Spérandio, M. (2015). A dynamic
672 physicochemical model for chemical phosphorus removal. *Water Research*, 73, 157-170.
- 673 Henze, M., Gujer, W., Mino, T. & van Loosdrecht, M.C.M. (2000). *Activated Sludge Models ASM1,
674 ASM2, ASM2d, and ASM3*. IWA Scientific and Technical Report No. 9. London, UK: IWA
675 Publishing.
- 676 Henze, M., van Loosdrecht, M.C.M. & Ekama, G.A. (2008). *Biological Wastewater Treatment: Principles,
677 Modeling, and Design*. London, UK: IWA Publishing.
- 678 ICIS (2016). *Indicative chemical prices A-Z*. Retrieved from <http://www.icis.com/chemicals/channel-info-chemicals-a-z/> [accessed 2016, July 14].
679

- 680 Ikumi, D.S., Brouckaert, C.J. & Ekama, G.A. (2011). Modelling of struvite precipitation in anaerobic
ACCEPTED MANUSCRIPT
681 digestion. In: Proceedings of Watermatex2011, San Sebastian, Spain, 20-22 June 2011.
- 682 Ikumi, D.S., Harding, T.H. & Ekama, G.A. (2014). Biodegradability of wastewater and activated sludge
683 organics in anaerobic digestion. *Water Research*, 56(1), 267-279.
- 684 Jaffer, Y., Clark, T.A., Pearce, P. & Parsons, S.A. (2002). Potential phosphorus recovery by struvite
685 formation. *Water Research*, 36(7), 1834-1842.
- 686 Jeppsson, U., Alex, J., Batstone, D., Benedetti, L., Comas, J., Copp, J.B., Corominas, L., Flores-Alsina, X.,
687 Gernaey, K.V., Nopens, I., Pons, M.-N., Rodriguez-Roda, I., Rosen, C., Steyer, J.-P., Vanrolleghem,
688 P.A., Volcke, E.I.P. & Vrecko, D. (2013). Benchmark simulation models, quo vadis?. *Water Science
689 & Technology*, 68(1), 1-15.
- 690 Jeppsson, U., Pons, M.N., Nopens, I., Alex, J., Copp, J.B., Gernaey, K.V., Rosen, C., Steyer, J.P. &
691 Vanrolleghem, P.A. (2007). Benchmark Simulation Model No 2 – general protocol and exploratory
692 case studies. *Water Science & Technology*, 56(8), 287-295.
- 693 Kazadi Mbamba, C., Flores-Alsina, X., Batstone, D.J. & Tait, S. (2015a). A generalised chemical
694 precipitation modelling approach in wastewater treatment applied to calcite. *Water Research*, 68, 342-
695 353.
- 696 Kazadi Mbamaba, C., Flores-Alsina, X., Batstone, D.J. & Tait, S. (2015b). A systematic study of multiple
697 minerals precipitation modelling in wastewater treatment. *Water Research*, 85, 359-70.
- 698 Kazadi Mbama, C., Flores-Alsina, X., Batstone, D.J. & Tait, S. (2016). Validation of a plant-wide modelling
699 approach with minerals precipitation in a full-scale WWTP. *Water Research*, 100, 169-183.
- 700 Krayzelova, L., Bartacek, J., Díaz, I., Jeison, D., Volcke, E.I.P. & Jenicek, P. (2015). Microaeration for
701 hydrogen sulfide removal during anaerobic treatment: a review. *Reviews on Environmental Science
702 and Biotechnology*, 14(4), 703-725.
- 703 Latif, M.A., Mehta, C.M. & Batstone, D.J. (2015). Low pH anaerobic digestion of waste activated sludge for
704 enhanced phosphorous release. *Water Research*, 81, 288-293.

- Lizarralde, I., Fernandez-Arevalo, T., Brouckaert, C., Vanrolleghem, P.A., Ikumi, D., Ekama, D., Ayesa, E. & Grau, P. (2015). A new general methodology for incorporating physico-chemical transformations into multiphase wastewater treatment process models. *Water Research*, 74, 239-256.
- Lopez-Vazquez, C.M., Hooijmans, C.M., Brdjanovic, D., Gijzen, H.J., & van Loosdrecht, M.C.M. (2007). A practical method for quantification of phosphorus- and glycogen-accumulating organism populations in activated sludge systems. *Water Environment Research*, 79(13), 2487-2498.
- Lopez-Vazquez, C.M., Oehmen, A., Hooijmans, C.M., Brdjanovic, D., Gijzen, H.J., Yuan, Z. & van Loosdrecht, M.C.M. (2009). Modeling the PAO-GAO competition: effects of carbon source, pH and temperature. *Water Research*, 43(2), 450-462.
- Luedecke, C., Hermanowicz, S.W. & Jenkins, D. (1989). Precipitation of ferric phosphate in activated sludge: A chemical model and its verification. *Water Science & Technology*, 21(4-5), 325-337.
- Mamais, D., Pitt, P.A., Cheng, Y.W., Loiacono, J. & Jenkins, D. (1994). Determination of ferric chloride dose to control struvite precipitation in anaerobic sludge digesters. *Water Environment Research*, 66(7), 912-918.
- Mannina, G., Ekama, G., Caniani, D., Cosenza, A., Esposito, G., Gori, R., Garrido-Baserba, M., Rosso, D. & Olsson, G. (2016). Greenhouse gases from wastewater treatment - A review of modelling tools. *Science of the Total Environment*, 551, 254-270.
- Marti, N., Pastor, L., Bouzas, A., Ferrer, J. & Seco, A. (2010). Phosphorus recovery by struvite crystallization in WWTPs: Influence of the sludge treatment line operation. *Water Research*, 44(7), 2371-2379.
- Marti, N., Ferrer, J., Seco, A. & Bouzas, A. (2008). Optimization of sludge line management to enhance phosphorus recovery in WWTP. *Water Research*, 42(18), 4609-4618.
- Martin, C. & Vanrolleghem, P.A. (2014). Analysing, completing, and generating influent data for WWTP modelling: A critical review. *Environmental Modelling & Software*, 60, 188-201.
- Münch, E.V. & Barr, K. (2001). Controlled struvite crystallisation for removing phosphorus from anaerobic digester sidestreams. *Water Research*, 35(1), 151-159.

- 731 Musvoto, E.V., Wentzel, M.C. & Ekama, G.A. (2000). Integrated chemical-physical processes modelling -
732 II. Simulating aeration treatment of anaerobic digester supernatants. *Water Research*, 34(6), 1868-
733 1880.
- 734 Ni, B.J., Peng, L., Law, Y., Guo, J. & Yuan, Z. (2014). Modeling of nitrous oxide production by autotrophic
735 ammonia-oxidizing bacteria with multiple production pathways. *Environmental Science &*
736 *Technology*, 48(7), 3916-3924.
- 737 Ni, B.J. & Yuan, Z. (2015). Recent advances in mathematical modeling of nitrous oxides emissions from
738 wastewater treatment processes. *Water Research*, 87, 336-346.
- 739 Nielsen, A. H., Lens, P., Vollertsen, J. & Hvitved-Jacobsen, T. (2005). Sulfide-iron interactions in domestic
740 wastewater from a gravity sewer. *Water Research*, 39(12), 2747-2755.
- 741 Nopens, I., Batstone, D.J., Copp, J.B., Jeppsson, U., Volcke, E., Alex, J. & Vanrolleghem, P.A. (2009). An
742 ASM/ADM model interface for dynamic plant-wide simulation. *Water Research*, 43(7), 1913-1923.
- 743 Nopens, I., Benedetti, L., Jeppsson, U., Pons, M.-N., Alex, J., Copp, J.B., Gernaey, K.V., Rosen, C., Steyer,
744 J.-P. & Vanrolleghem, P.A. (2010). Benchmark Simulation Model No 2 – Finalisation of plant layout
745 and default control strategy. *Water Science & Technology*, 62(9), 1967-1974.
- 746 Oehmen, A., Lopez-Vazquez, C.M., Carvalho, G., Reis, M.A.M. & van Loosdrecht, M.C.M. (2010).
747 Modelling the population dynamics and metabolic diversity of organisms relevant in
748 anaerobic/anoxic/aerobic enhanced biological phosphorus removal processes. *Water Research*, 44(15),
749 4473-4486.
- 750 Otterpohl, R. & Freund, M. (1992). Dynamic models for clarifiers of activated sludge plants with dry and
751 wet weather flows. *Water Science & Technology*, 26(5-6), 1391-1400.
- 752 Pikaar, I., Sharma, K. R., Hu, S., Gernjak, W., Keller, J., & Yuan, Z. (2014). Reducing sewer corrosion
753 through integrated urban water management. *Science*, 345(6198), 812-814.
- 754 Pokorna-Krayzelova, L., Mampaey, K.E., Vannecke, T.P.W., Bartacek, J., Jenicek, P. & Volcke, E.I.P.
755 (2017). Model-based optimization of microaeration for biogas desulfurization in UASB reactors.
756 (submitted)

- 757 Prasad, M.N.V. & Shih, K. (2016). *Environmental Materials and Waste: Resource Recovery and Pollution*
758 *Prevention*. London, UK: Elsevier Inc.
- 759 Rieger, L., Alex, J., Winkler, S., Boehler, M., Thomann, M. & Siegrist, H. (2003). Progress in sensor
760 technology - progress in process control Part I: Sensor property investigation and classification. *Water*
761 *Science & Technology*, 47(2), 103-112.
- 762 Romero-Güiza, M.S., Tait, S., Astals, S., Del Valle-Zermeño, R., Martínez, M., Mata-Alvarez, J. &
763 Chimenos, J.M. (2015). Reagent use efficiency with removal of nitrogen from pig slurry via struvite:
764 A study on magnesium oxide and related by-products. *Water Research*, 84, 286-294.
- 765 Rosen, C., Vrecko, D., Gernaey, K.V., Pons, M.-N. & Jeppsson, U. (2006). Implementing ADM1 for plant-
766 wide benchmark simulations in Matlab/Simulink. *Water Science & Technology*, 54(4), 11-19.
- 767 Ruano, M.V., Serralta, J., Ribes, J., Garcia-Usach, F., Bouzas, A. & Barat, R. (2011). Application of the
768 general model Biological Nutrient Removal Model No. 1 to upgrade two full-scale WWTPs.
769 *Environmental Technology*, 33(9), 1005-1012.
- 770 Serralta, J., Borrás, L. & Seco, A. (2004). An extension of ASM2d including pH calculation. *Water*
771 *Research*, 38(19), 4029-4038.
- 772 Shu, L., Schneider, P., Jegatheesan, V. & Johnson, J. (2006). An economic evaluation of phosphorus
773 recovery as struvite from digester supernatant. *Bioresource Technology*, 97(17), 2211-2216.
- 774 Siegrist, H., Brunner, I., Koch, G., Con Phan, L. & Van Chieu, L. (1999). Reduction of biomass decay under
775 anoxic and anaerobic conditions. *Water Science & Technology*, 39(1), 129-137.
- 776 Skogestad, S. (2000). Plantwide control: the search for the self-optimizing control structure. *Journal of*
777 *Process Control*, 10, 487-507.
- 778 Snip, L., Flores-Alsina, X., Plósz, B.G., Jeppsson, U. & Gernaey, K.V. (2014). Modelling the occurrence,
779 transport and fate of pharmaceuticals in wastewater systems. *Environmental Modelling & Software*,
780 62, 112-127.
- 781 Snip, L.J.P., Flores-Alsina, X., Aymerich, I., Rodríguez-Mozaz, S., Barceló, D., Plósz, B.G., Corominas, L.,
782 Rodríguez-Roda, I., Jeppsson, U. & Gernaey, K.V. (2016). Generation of synthetic data to perform

- Solon, K., Flores-Alsina, X., Kazadi Mbamba, C., Volcke, E.I.P., Tait, S., Batstone, D.J., Gernaey, K.V. & Jeppsson, U. (2015). Effects of ionic strength and ion pairing on (plant-wide) modelling of anaerobic digestion processes. *Water Research*, 70, 235-245.
- Stumm, W. & Morgan, J.J. (1996). *Aquatic Chemistry: Chemical Equilibria and Rates in Natural Waters*. Schnoor, J.L., Zehnder, A. (Eds.). New York, NY, USA: John Wiley and Sons.
- Sweetapple, C.G. (2015). *Developing Strategies for the Reduction of Greenhouse Gas Emissions from Wastewater Treatment*. PhD thesis, University of Exeter, UK.
- Takács, I., Patry, G.G. & Nolasco, D. (1991). A dynamic model of the clarification thickening process. *Water Research*, 25(10), 1263-1271.
- Tchobanoglous, G., Burton, F.L. & Stensel, H.D. (2003). *Wastewater Engineering: Treatment and Reuse* (4th ed.). Boston, Massachusetts, USA: McGraw-Hill Education.
- Truskey, G., Yuan, F. & Katz, D.F. (2009). *Transport Phenomena in Biological Systems*. Upper Saddle River, New Jersey, USA: Prentice Hall.
- Vaneckhaute, C. (2015). *Nutrient Recovery from Bio-digestion Waste: from Field Experimentation to Model-based Optimization*. PhD thesis, Université Laval, Québec, Canada.
- Vaneckhaute, C., Lebuf, V., Michels, E., Belia, E., Vanrollegem, P.A., Tack, F.M.G. & Meers, E. (2017). Nutrient recovery from digestate: Systematic technology review and product classification. *Waste Biomass Valorization*, 8(1), 21-40.
- van Rensburg, P., Musvoto, E.V., Wentzel, M.C. & Ekama, G.A. (2003). Modelling multiple mineral precipitation in anaerobic digester liquor. *Water Research*, 37(13), 3087-3097.
- Vanrollegem, P.A., Corominas, L. & Flores-Alsina, X. (2010). Real-time control and effluent ammonia violations induced by return liquor overloads. In: *Proceedings of the Water Environment Federation*, 2010(9), 7101-7108.
- Vanrollegem, P.A., Flores-Alsina, X., Guo, L., Solon, K., Ikumi, D., Batstone, D.J., Brouckaert, C., Takács, I., Grau, P., Ekama, G.A., Jeppsson, U. & Gernaey, K.V. (2014). Towards BSM2-GPS-X: A

- 810 plant-wide benchmark simulation model not only for carbon and nitrogen, but also for greenhouse
811 gases (G), phosphorus (P), sulphur (S) and micropollutants (X), all within the fence of
812 WWTPs/WRRFs. In: Proceedings of the IWA/WEF Wastewater Treatment Modelling Seminar, Spa,
813 Belgium, 30 March-2 April 2014.
- 814 Vanrolleghem, P.A. & Vaneckhaute, C. (2014). Resource recovery from wastewater and sludge: Modelling
815 and control challenges. In: Proceedings of the IWA Specialist conference on Global Challenges for
816 Sustainable Wastewater Treatment and Resource Recovery, Kathmandu, Nepal, 26-30 October 2014.
- 817 Verstraete, W., Van de Caveye, P. & Diamantis, V. (2009). Maximum use of resources present in domestic
818 “used water”. *Bioresource Technology*, 100(23), 5537-5545.
- 819 Volcke, E.I.P., Gernaey, K.V., Vrecko, D., Jeppsson, U., van Loosdrecht, M.C.M. & Vanrolleghem P.A.
820 (2006a). Plant-wide (BSM2) evaluation of reject water treatment with a SHARON-Anammox process.
821 *Water Science & Technology*, 54(8), 93-100.
- 822 Volcke, E.I.P., van Loosdrecht, M.C.M. & Vanrolleghem, P.A. (2006b). Continuity-based model interfacing
823 for plant-wide simulation: A general approach. *Water Research*, 40(15), 2817-2828.
- 824 Wang, R., Yongmei, L., Chen, W., Zou, J. & Chen, Y. (2016). Phosphate release involving PAOs activity
825 during anaerobic fermentation of EBPR sludge and the extension of ADM1. *Chemical Engineering*
826 *Journal*, 297(1), 436-447.
- 827 Wentzel, M., Ekama, G. & Sotemann, S. (2006). Mass balance based plant wide treatment model – Part 1.
828 Biodegradability of wastewater organics under anaerobic conditions. *Water SA*, 32(3), 2692-2675.
- 829 Xu, X., Chen, C., Lee, D.J., Wang, A., Guo, W., Zhou, X., Guo, H., Yuan, Y., Ren, N. & Chang, J.S. (2013).
830 Sulfate-reduction, sulfide-oxidation and elemental sulfur bioreduction process: modeling and
831 experimental validation. *Bioresource Technology*, 147, 202-211.
- 832 Zaher, U., Grau, P., Benedetti, L., Ayesa, E. & Vanrolleghem, P.A. (2007). Transformers for interfacing
833 anaerobic digestion models to pre- and post-treatment processes in a plant-wide modelling context.
834 *Environmental Modelling & Software*, 22(1), 40-58.

835 Zhang, J., Zhang, Y., Chang, J., Quan, X. & Li, Q. (2013). Biological sulfate reduction in the acidogenic
836 phase of anaerobic digestion under dissimilatory Fe (III)-reducing conditions. *Water Research*, 47(6),
837 2033-2040.

838

839

ACCEPTED MANUSCRIPT

Table 1. Main characteristics of the implemented control/operational strategies

Characteristics	DO controller	Ammonium controller	TSS controller	Phosphate controller	Airflow in STRIP	Magnesium controller
Measured variable(s)	S_{O_2} in AER2	S_{NH_x} in AER2	TSS in AER3	S_{PO_4} in AER3	-	-
Controlled Variable(s)	S_{O_2} in AER2	S_{O_2} in AER1, 2 & 3	TSS in AER3	S_{PO_4} in AER3	S_{CO_2} in STRIP	$X_{Mg(OH)_2}$ in STRIP
Set point/critical value	-	$2 \text{ g N}\cdot\text{m}^{-3}$	$4000 \text{ g TSS}\cdot\text{m}^{-3}$ (if $T < 15^\circ\text{C}$) $3000 \text{ g TSS}\cdot\text{m}^{-3}$ (if $T > 15^\circ\text{C}$)	$1 \text{ g P}\cdot\text{m}^{-3}$	-	-
Manipulated variable	Q_{air} in AER1, 2 & 3	S_{O_2} set point in AER2	Q_w	Q_{FeCl_3}	$Q_{stripping}$	$Q_{Mg(OH)_2}$
Control algorithm	PI	Cascade PI	Cascade PI	PI	-	-
Applied in control strategies A_i	A_1, A_2 & A_3	A_1, A_2 & A_3	A_1, A_2 & A_3	A_2	A_3	A_3

Table 2. Evaluation criteria for the three evaluated control/operational strategies

Operational alternatives →	default	A_1	A_2	A_3	
N_{Kjeldahl}	3.5	3.6	3.6	3.7	g N.m^{-3}
N_{total}	11.2	9.2	9.1	8.5	g N.m^{-3}
P_{inorg}	5.95	2.9	0.9	0.6	g P.m^{-3}
P_{total}	6.4	3.7	1.7	1.5	g P.m^{-3}
E_{QI}	18 234	12 508	8237	7766	$\text{kg pollution.d}^{-1}$
$TIV S_{\text{NH}_x}$ (= 4 g N.m ⁻³)	0.95	0.07	0.08	0.08	%
$TIV N_{\text{total}}$ (= 14 g N.m ⁻³)	0	0	0	0	%
$TIV P_{\text{total}}$ (= 2 g P.m ⁻³)	100	75	13.4	15.7	%
E_{aeration}	4000	3146	3218	3194	kWh.d^{-1}
$E_{\text{production}}^1$	5955	6054	6150	6038	kWh.d^{-1}
SP_{disposal}^2	3461	3538	3730	3487	kg TSS.d^{-1}
Q_{FeCl_3}	-	-	169	-	kg Fe.d^{-1}
$Q_{\text{Mg(OH)}_2}$	-	-	-	40	kg Mg.d^{-1}
$S_{\text{recovered}}^3$	-	-	-	206	$\text{kg struvite.d}^{-1}$
OCI^4	10 201	9495	13 770	8912	-
G_{CH_4}	992	1009	1025	1006	$\text{kg CH}_4.\text{d}^{-1}$
$G_{\text{H}_2\text{S}}$	17.4	19.2	12.1	19.2	$\text{kg H}_2\text{S.d}^{-1}$
N_{removed}/OCI	0.079	0.089	0.062	0.097	$\text{kg N (removed).OCI}^{-1}$
P_{removed}/OCI	0.007	0.013	0.012	0.019	$\text{kg P (removed).OCI}^{-1}$

¹ The electricity generated by the turbine is calculated by using a factor for the energy content of the methane gas (50.014 MJ (kg CH₄)⁻¹) and assuming 43 % efficiency for electricity generation.

² SP_{disposal} refers to the amount of solids which accumulate in the plant over the time of evaluation combined with the amount of solids removed from the process (i.e. dewatered sludge). See **Gernaey et al. (2014)** for a more detailed description.

³ $S_{\text{recovered}}$ refers to the amount of recovered struvite. See Supplemental Information for a more detailed description.

⁴ Relative costs for chemicals are calculated assuming 2400 \$/ton as Fe (**ICIS, 2016**), 600 \$/ton as Mg (**ICIS, 2016**) and 200 \$/ton as struvite (value) (**Prasad & Shih, 2016; Jaffer et al., 2002; Münch and Barr, 2001**).

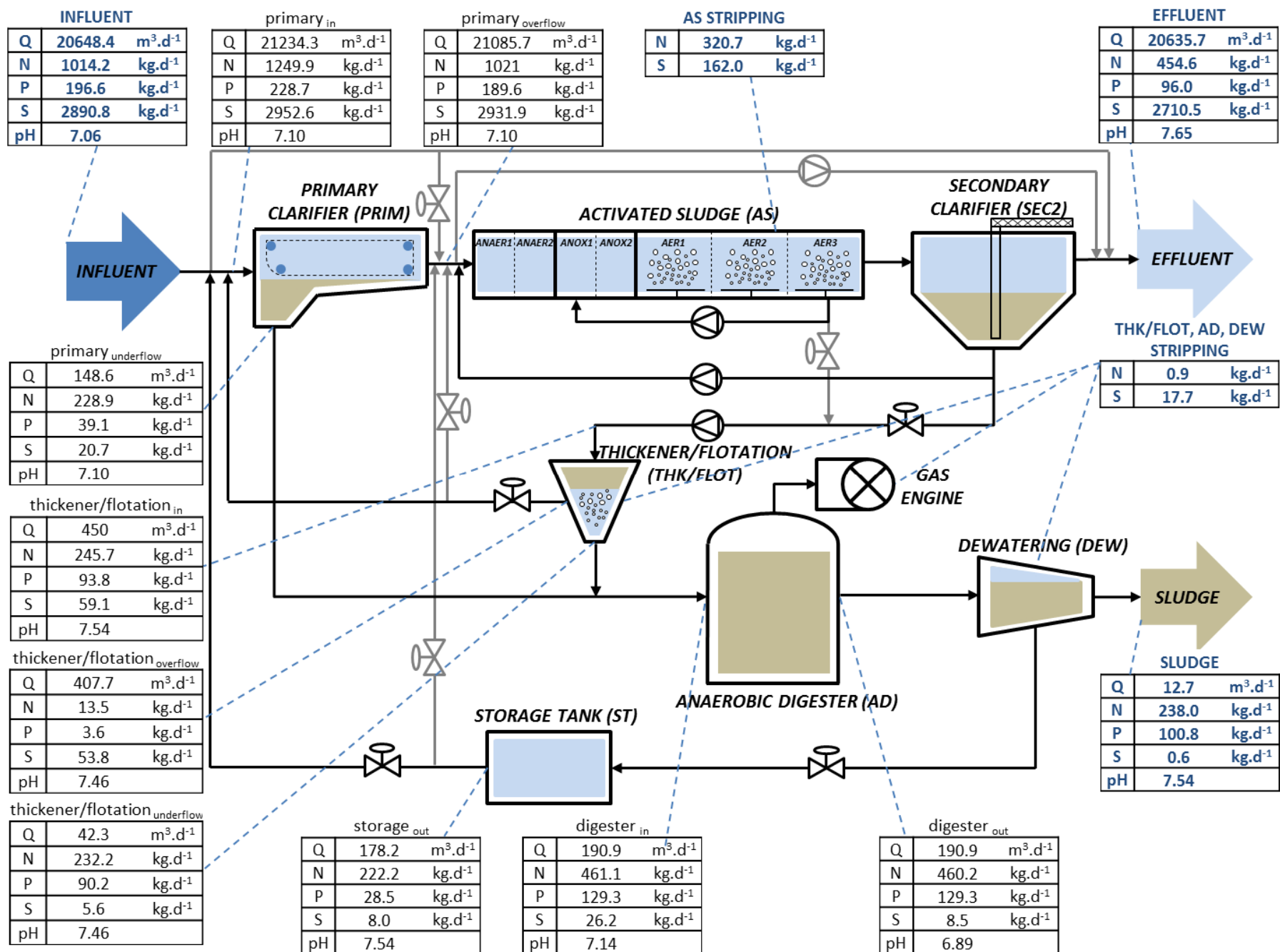


Figure 1. Block flow diagram including overall and individual (N, P, S, pH) balances for the WWTP under study (scenario A_0).

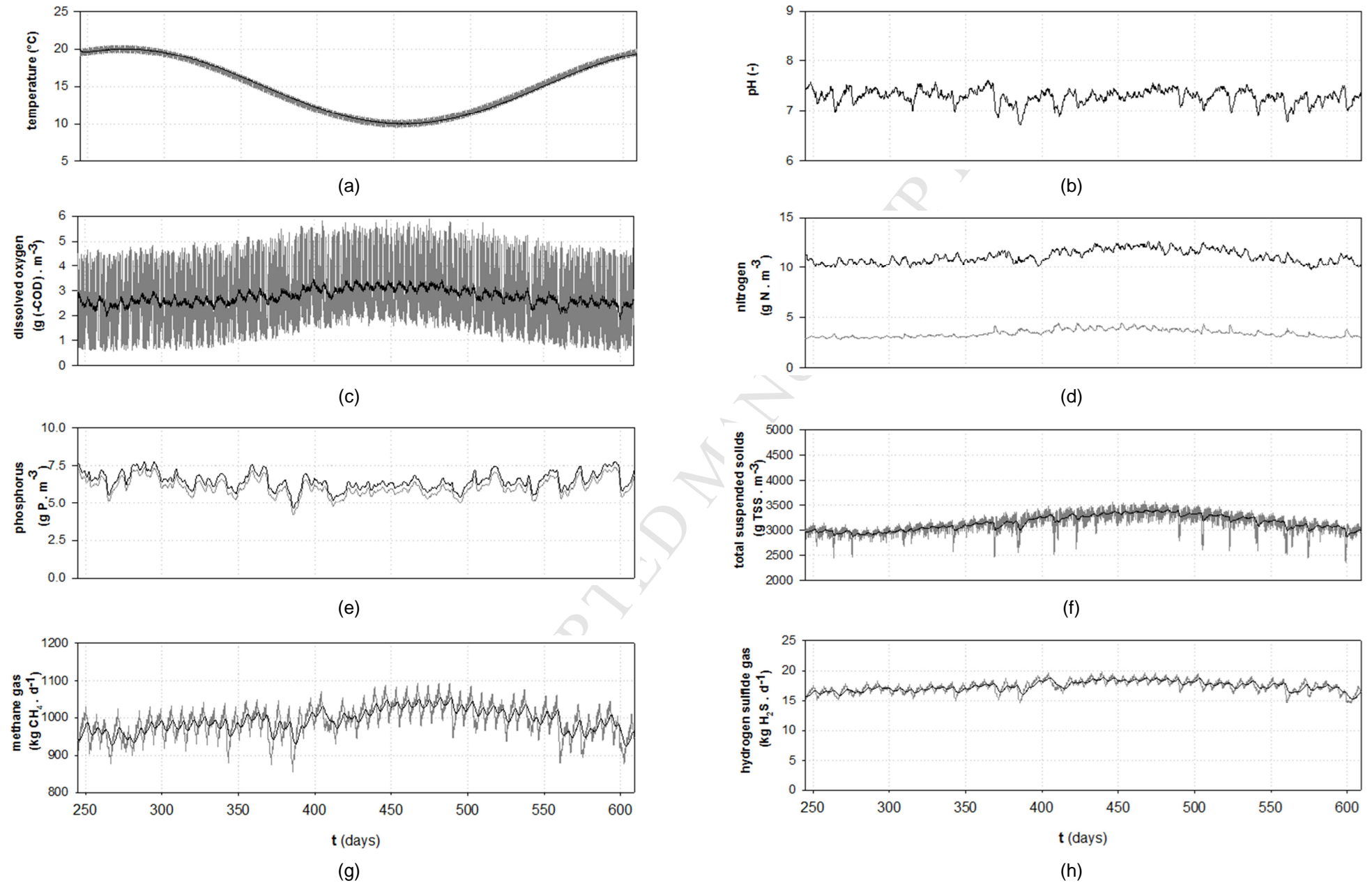


Figure 2. Dynamic profiles (A_0 = open loop) for: (a) influent temperature; (b) influent pH; (c) dissolved oxygen in AER2; (d) effluent N (S_{NH_x} (grey) and TN (black)); (e) effluent P (S_{IP} (grey) and TP (black)); (f) TSS in AER3; (g) methane gas production; and, (h) hydrogen sulfide gas production. Simulation time is one year. A 3-day exponential filter is used to improve visualization of the results. Raw data is presented in grey (in (a), (b), (c), (f), (g) and (h)).

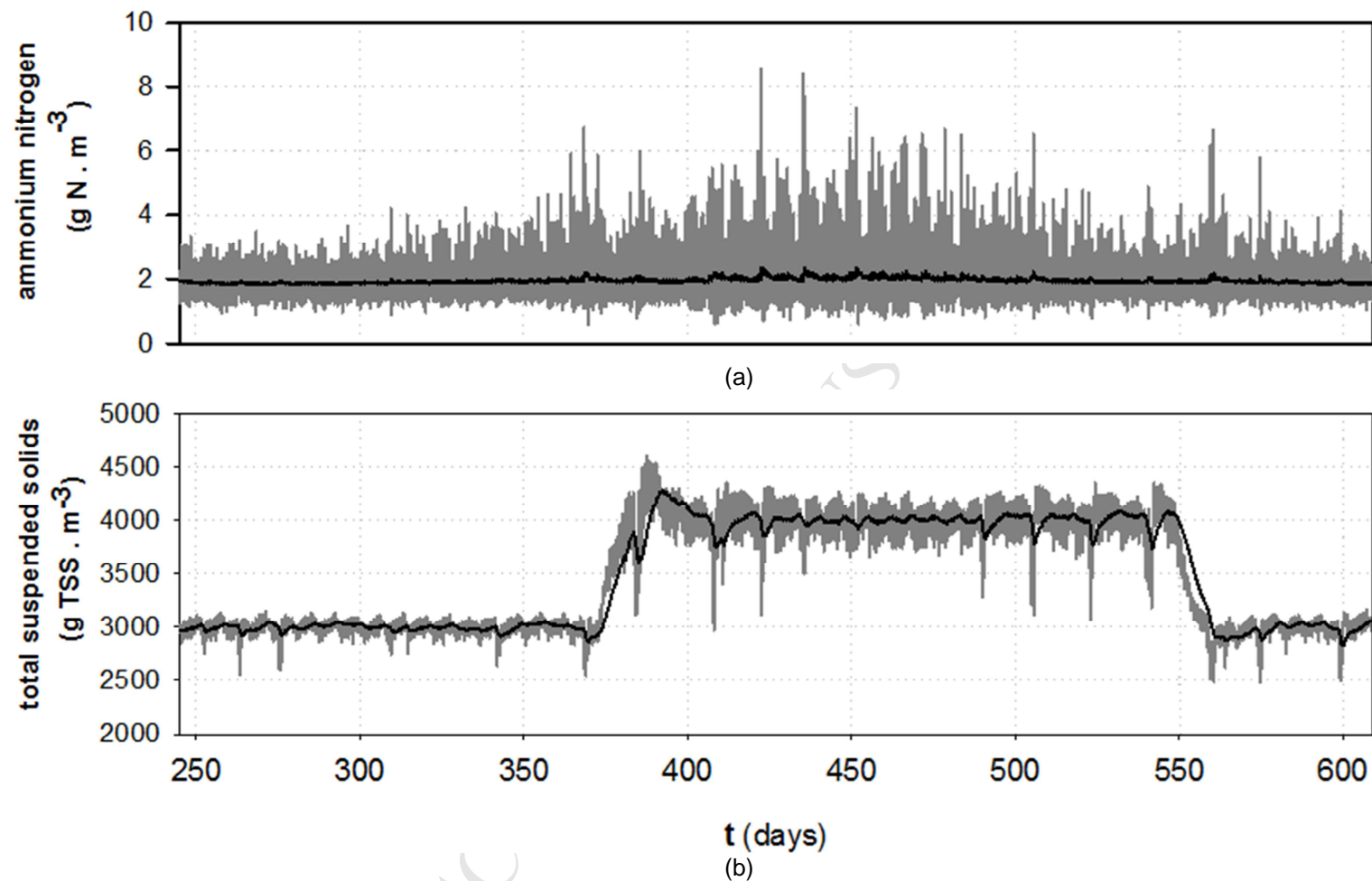


Figure 3. Dynamic profiles (A_1) of: (a) S_{NH_x} in AER2; and, (b) X_{TSS} in AER3 after implementing alternative A_1 . A 3-day exponential filter is used to improve visualization of the results. Raw data is presented in grey. (Note that $T < 15^\circ\text{C}$ starts on day 357 and lasts until day 549).

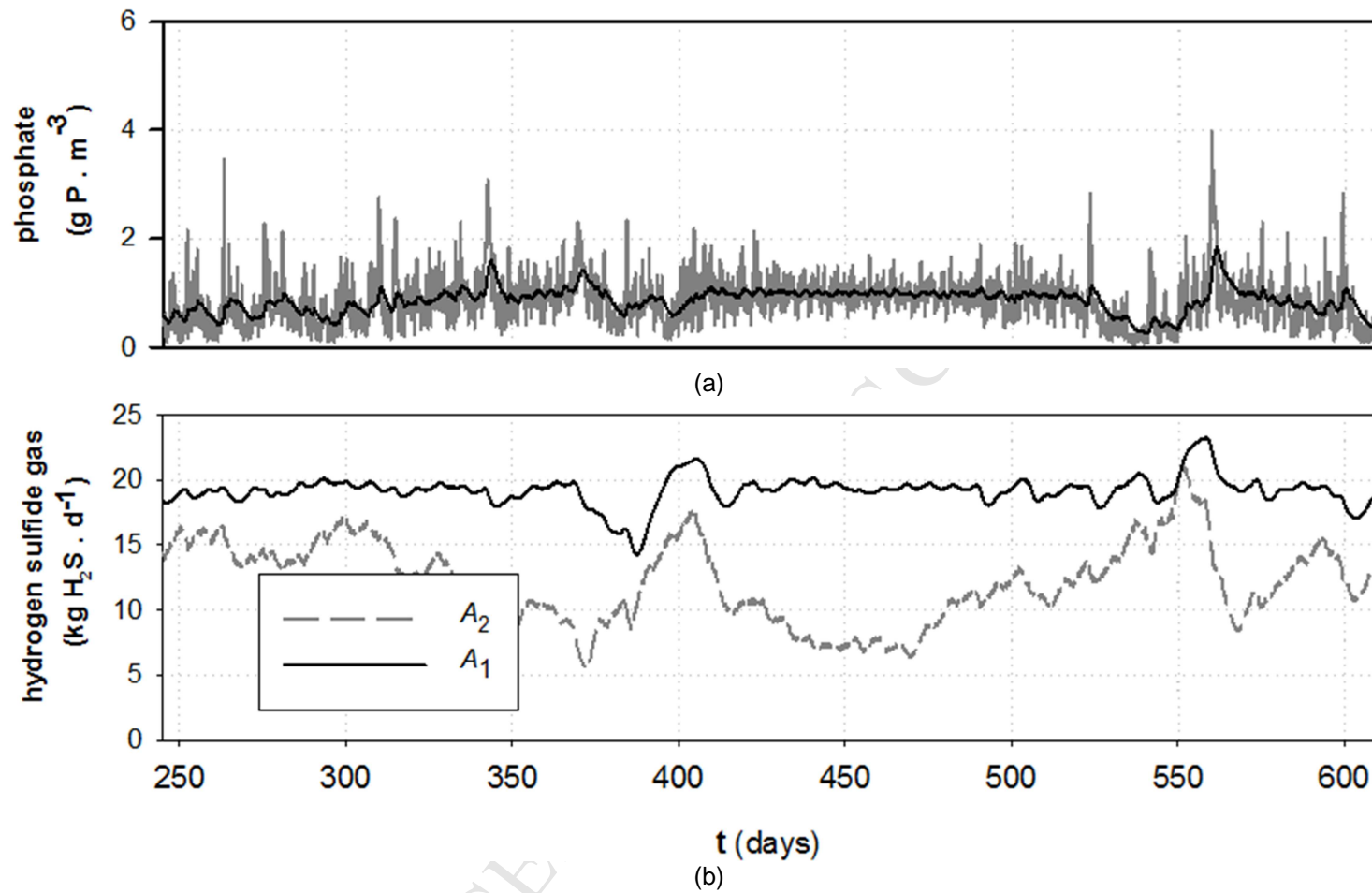


Figure 4. Dynamic profiles (A_2) of: (a) S_{PO_4} in AER3; and, (b) $G_{\text{H}_2\text{S}}$ in the AD after implementing alternative A_2 . A 3-day exponential filter is used to improve visualization of the results. Raw data is presented in grey.

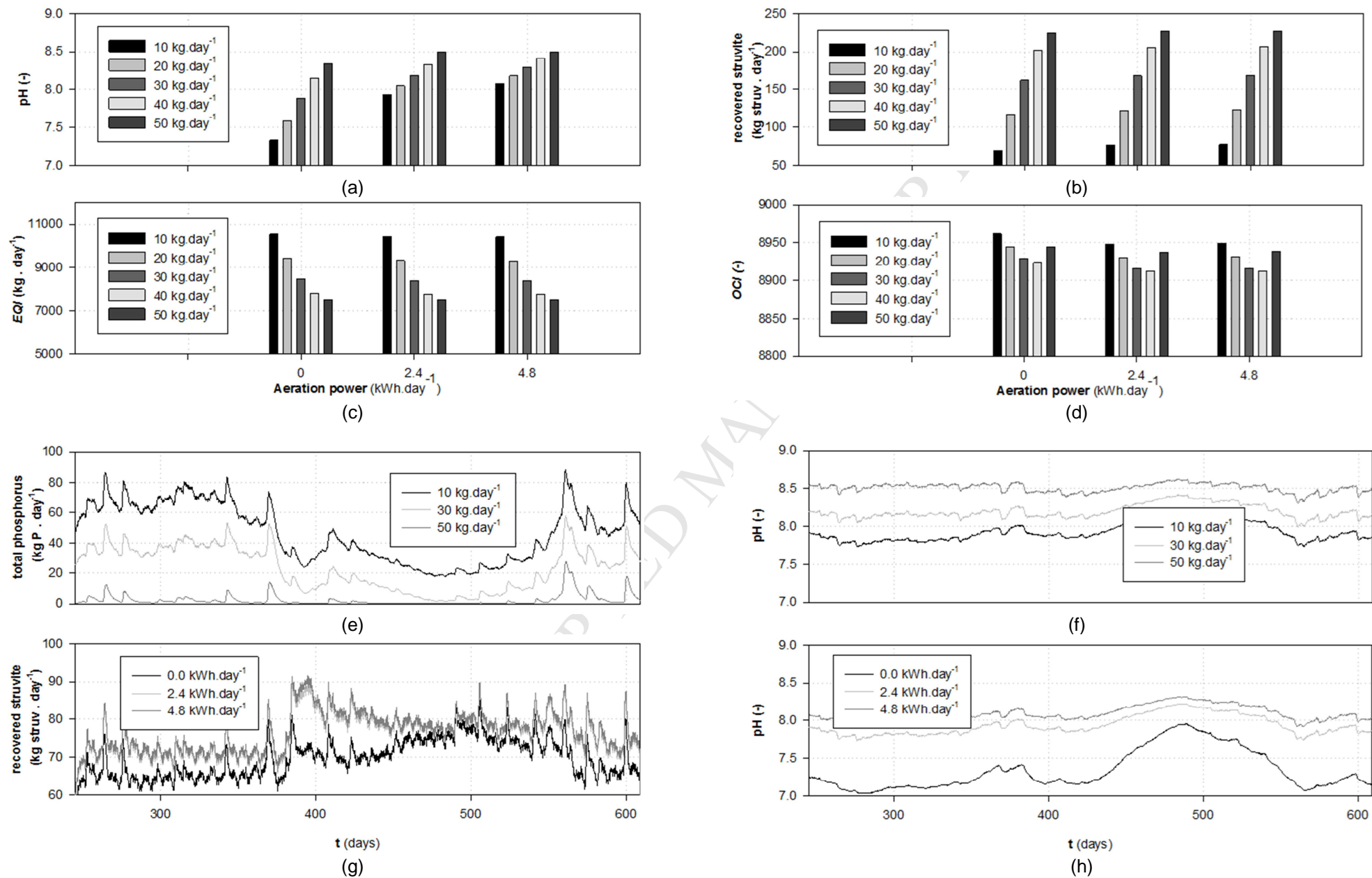


Figure 5. Effect of aeration power $Q_{stripping}$ /dosage addition $Q_{Mg(OH)_2}$ on (a), (f), (h): pH in the stripping unit (STRIP); (b), (g): quantity of recovered struvite; (c) EQI; (d) OCI; and, (e) P content in the anaerobic digester supernatant. A 3-day exponential filter is used to improve visualization of the results in (e), (f), (g) and (h).

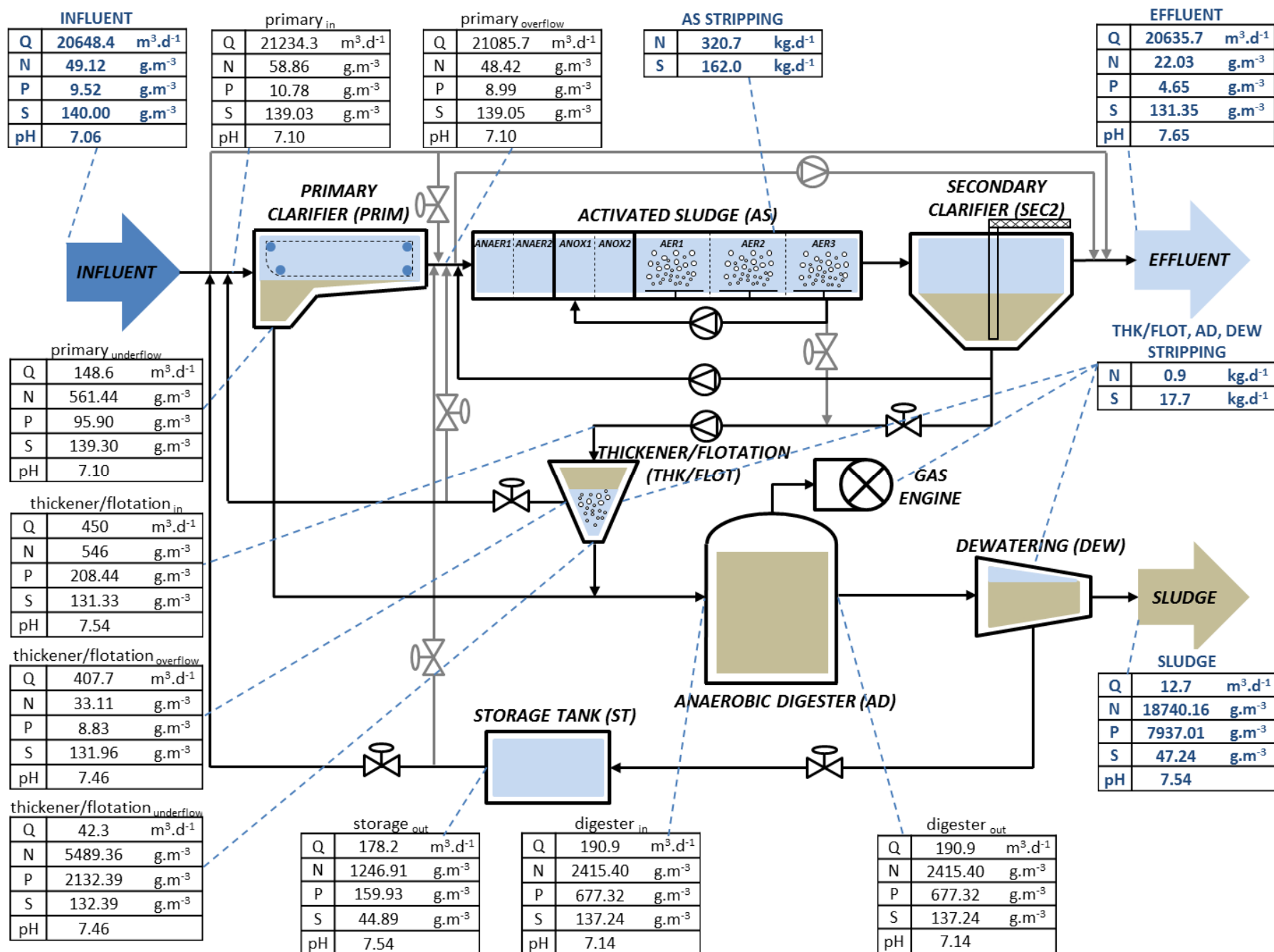


Figure SS1. Block flow diagram including overall and individual (N, P, S, pH) concentrations for the WWTP under study (scenario A₀).

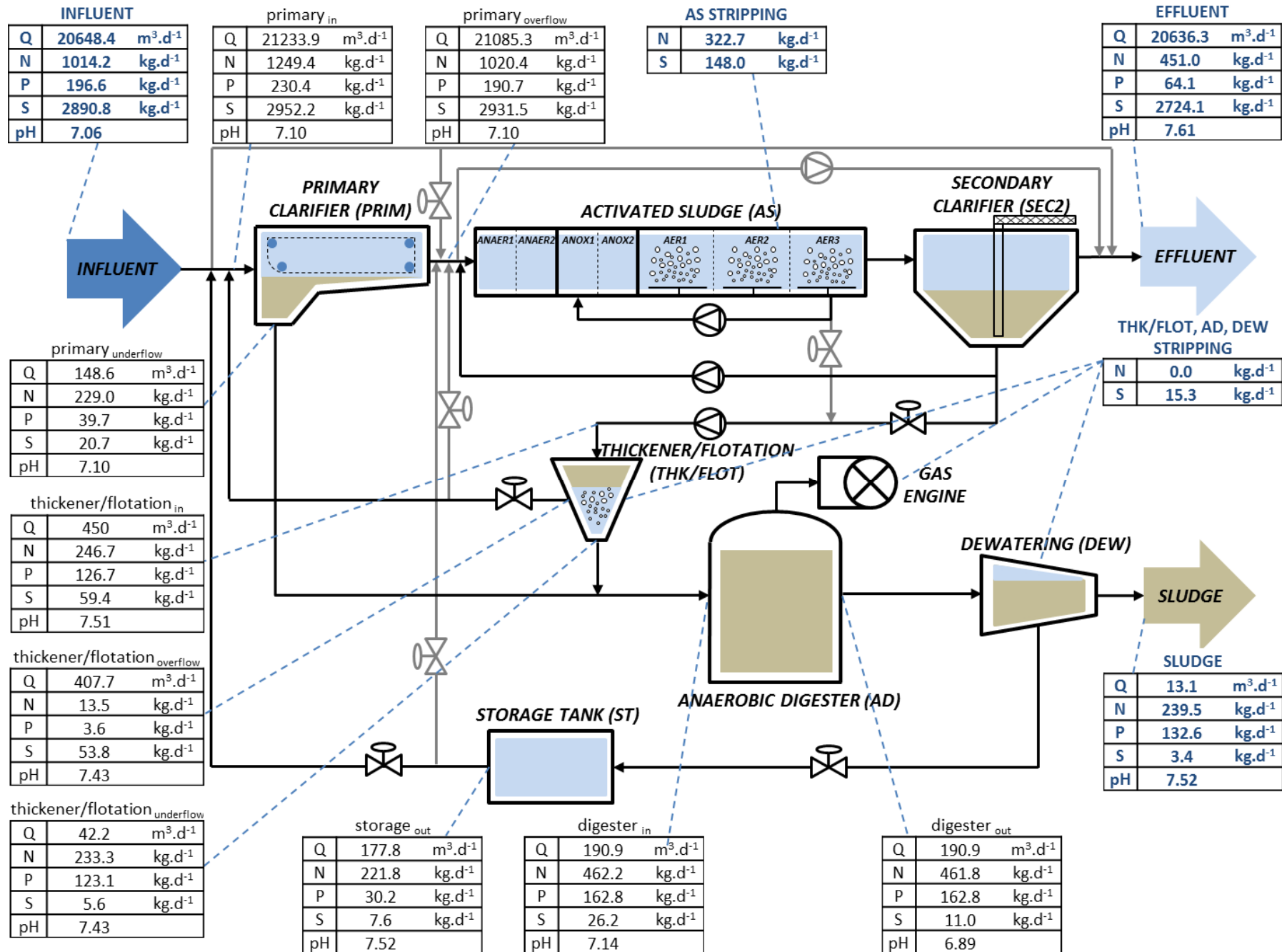


Figure SS2. Block flow diagram including overall and individual (N, P, S, pH) balances for the WWTP under study (scenario A_2).

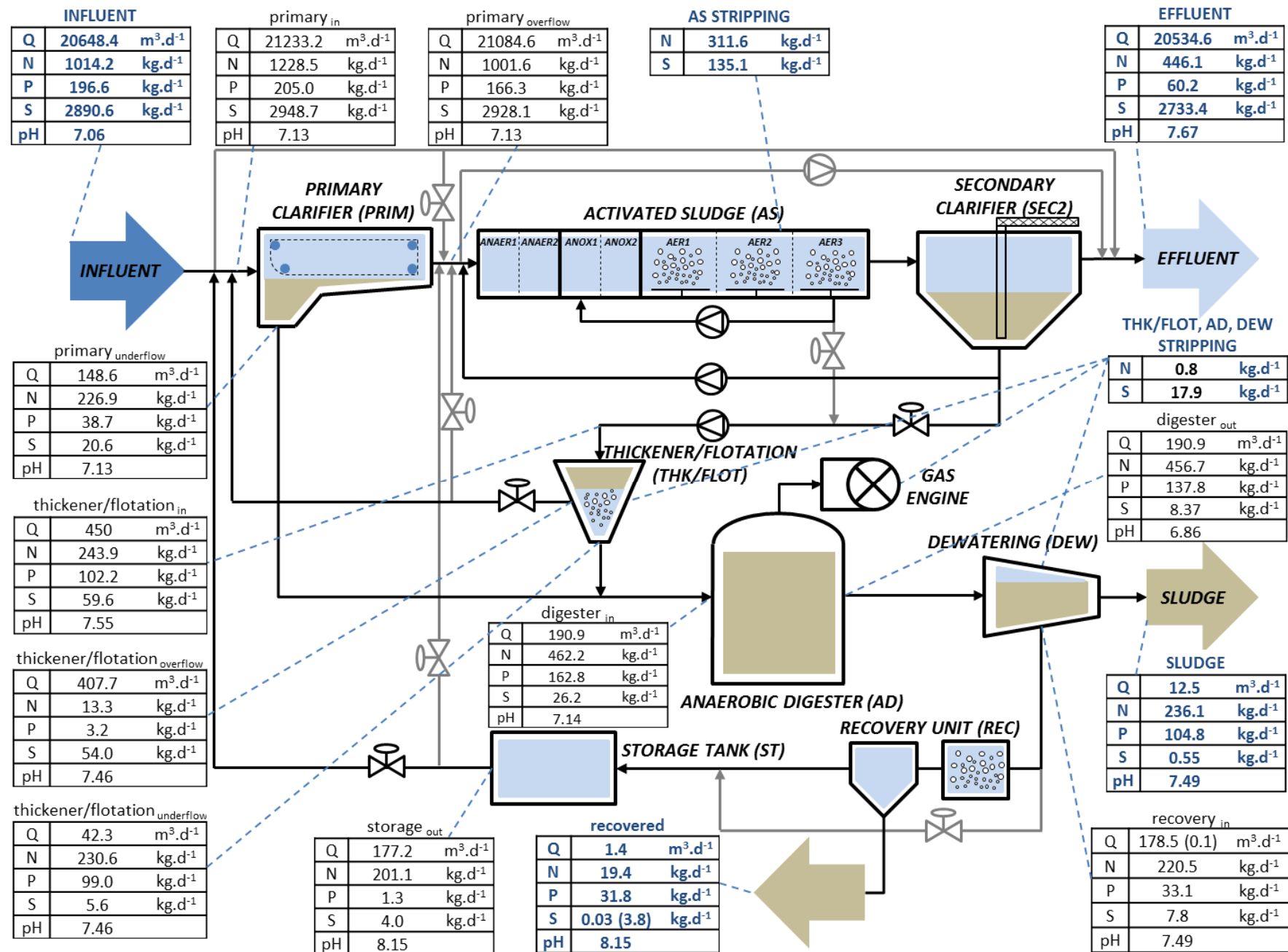


Figure SS3. Block flow diagram including overall and individual (N, P, S, pH) balances for the WWTP under study (scenario A₃).

Values in between parentheses represent: H₂S gas that is stripped (REC) and minor flow due to metal addition (DEW).

Plant-wide modelling of phosphorus transformations in wastewater treatment systems: Impacts of control and operational strategies

K. Solon¹, X. Flores-Alsina², C. Kazadi Mbamba³, D. Ikumi⁴, E.I.P. Volcke⁵, C. Vaneckhaute⁶, G. Ekama⁴, P.A. Vanrolleghem⁷, D.J. Batstone³, K.V. Gernaey², U. Jeppsson^{1*}

¹ Division of Industrial Electrical Engineering and Automation, Department of Biomedical Engineering, Lund University, Box 118, SE-221 00 Lund, Sweden.

² CAPEC-PROCESS Research Center, Department of Chemical and Biochemical Engineering, Technical University of Denmark, Building 229, DK-2800 Kgs. Lyngby, Denmark.

³ Advanced Water Management Centre, The University of Queensland, St Lucia, Brisbane, Queensland 4072, Australia.

⁴ Water Research Group, Department of Civil Engineering, University of Cape Town, Rondebosch 7700, South Africa.

⁵ Department of Biosystems Engineering, Ghent University, Coupure links 653, B-9000 Gent, Belgium.

⁶ BioEngine, Department of Chemical Engineering, Université Laval, Québec, QC, Canada, G1V 0A6.

⁷ modelEAU, Département de Génie Civil et de Génie des Eaux, Université Laval, Québec, QC, Canada, G1V 0A6.

**Corresponding author:*

Ulf Jeppsson

Division of Industrial Electrical Engineering and Automation (IEA)

Department of Biomedical Engineering

Lund University, Box 118, SE-221 00

Lund, Sweden

Phone: +46 46 222 92 87

Fax: +46 46 14 21 14

e-mail: ulf.jeppsson@iea.lth.se

RESEARCH HIGHLIGHTS

- Development of a plant-wide model describing P (together with N, S, Fe), including pH prediction
- Operational strategies, such as aeration control and dosing of metals, have complex plant-wide interactions
- Quantification of overall and individual N, P, S mass balances through the different process units
- Multi-criteria (economic/environmental) analysis of the evaluation results